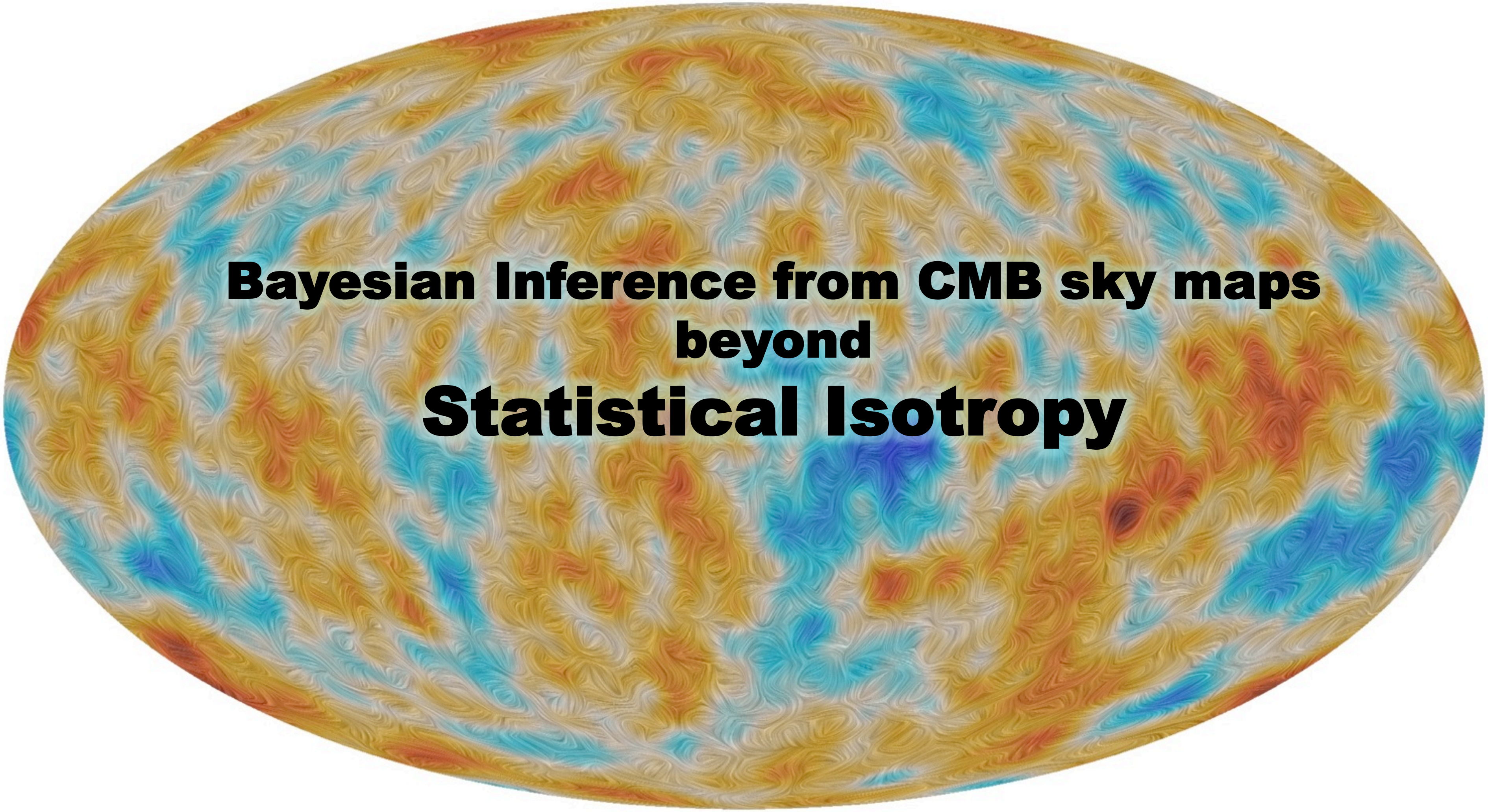

Bayesian Inference from CMB sky maps beyond Statistical Isotropy

CosKASI Conference 2017
Cosmological quests for the next decade

KASI, Daejeon, Korea
Apr. 17-21, 2017

Tarun Souradeep
IUCAA, Pune, India

Suvodip Mukherjee, Santanu Das, Aditya Rotti, Nidhi Pant, Pavan Aluri, Shabbir Shaikh, Rajorshi Chanda, Debabrata Adak

Cosmic “Super–IMAX” theater

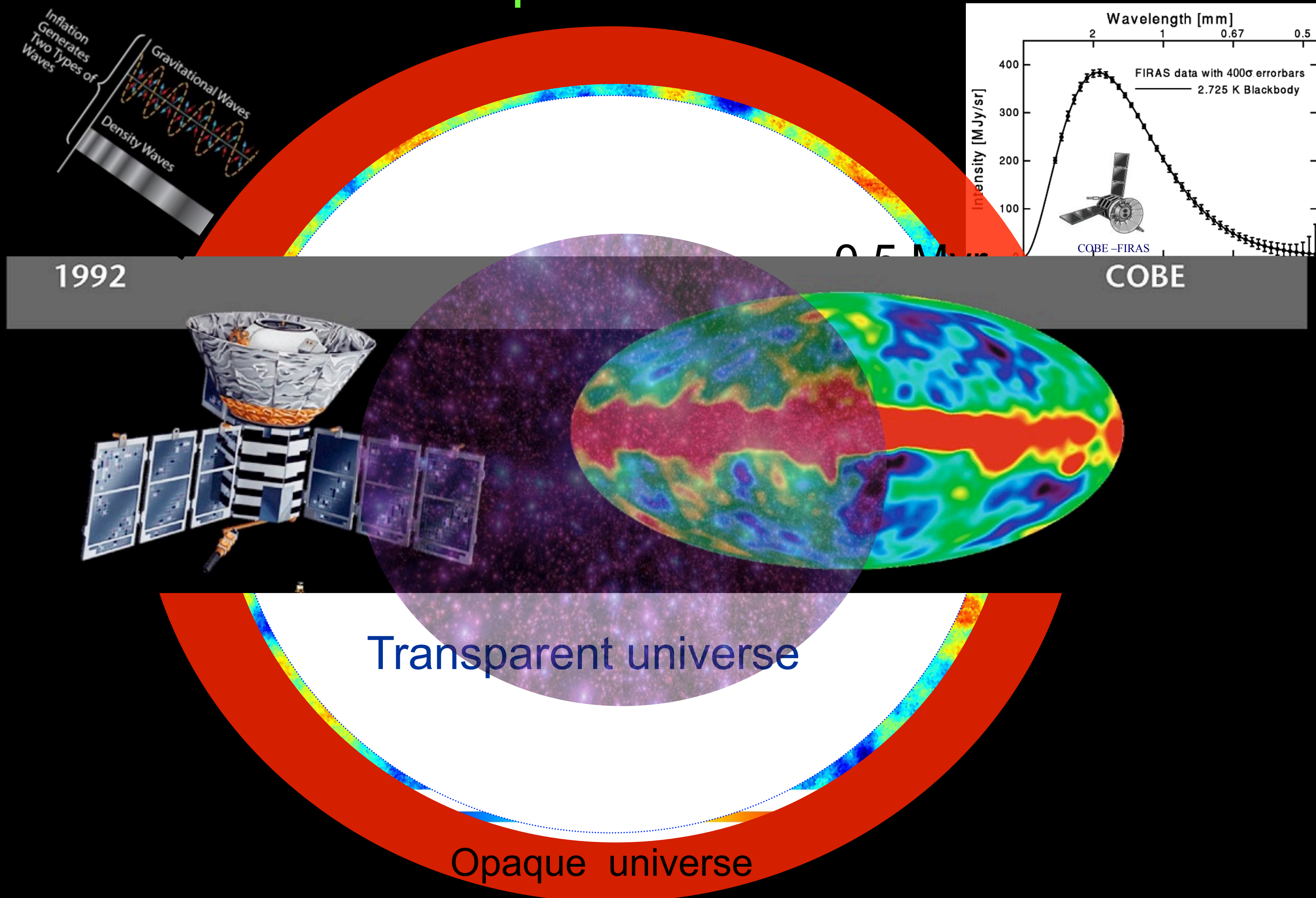

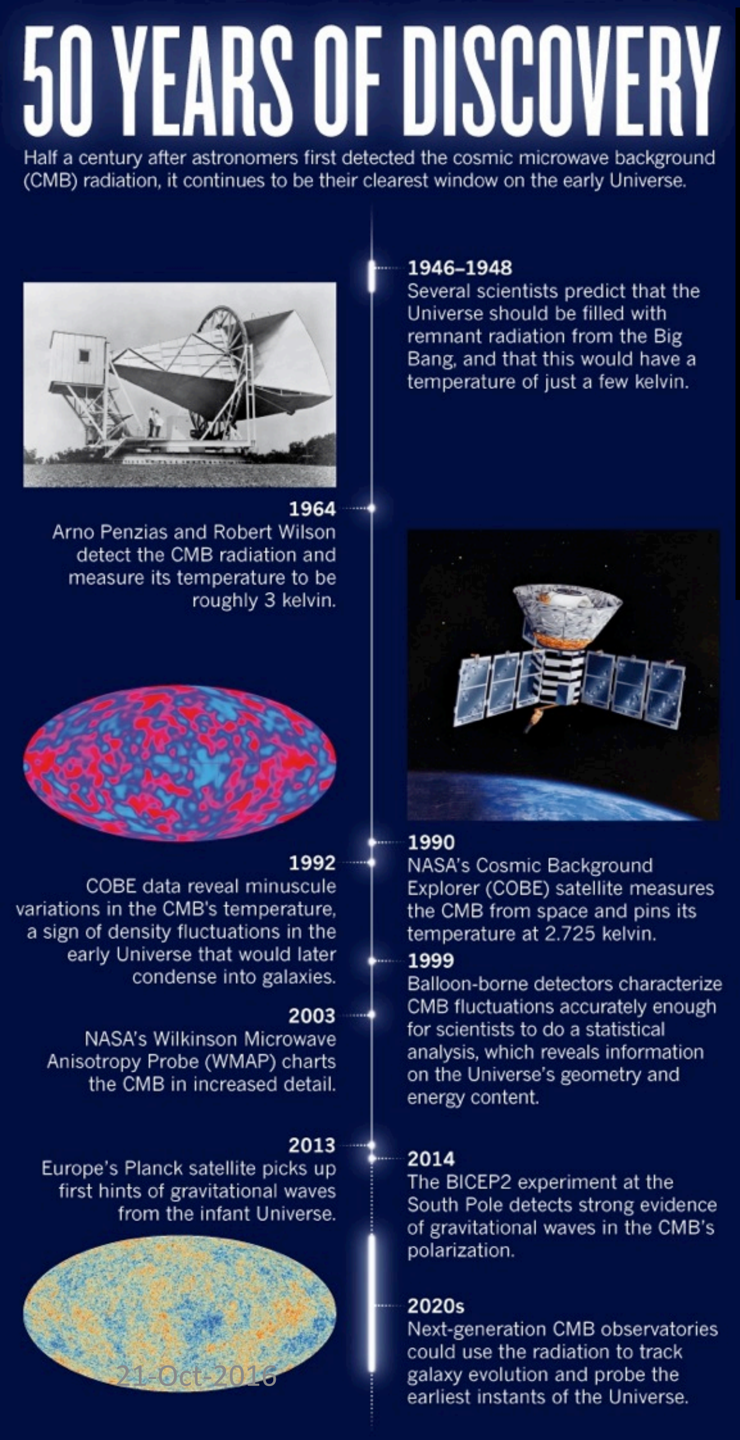
50 YEARS OF DISCOVERY
Half a century after astronomers first detected the cosmic microwave background (CMB) radiation, it continues to be their clearest window on the early Universe.
1946–1948
Several scientists predict that the Universe should be filled with remnant radiation from the Big Bang, and that this would have a temperature of just a few kelvin.
1964
Arno Penzias and Robert Wilson detect the CMB radiation and measure its temperature to be roughly 3 kelvin.
1990
NASA's Cosmic Background Explorer (COBE) satellite measures the CMB from space and pins its temperature at 2.725 kelvin.
1992
COBE data reveal minuscule variations in the CMB's temperature, a sign of density fluctuations in the early Universe that would later condense into galaxies.
1999
Balloon-borne detectors characterize CMB fluctuations accurately enough for scientists to do a statistical analysis, which reveals information on the Universe's geometry and energy content.
2003
NASA's Wilkinson Microwave Anisotropy Probe (WMAP) charts the CMB in increased detail.
2013
Europe's Planck satellite picks up first hints of gravitational waves from the infant Universe.
2014
The BICEP2 experiment at the South Pole detects strong evidence of gravitational waves in the CMB's polarization.
2020s
Next-generation CMB observatories could use the radiation to track galaxy evolution and probe the earliest instants of the Universe.

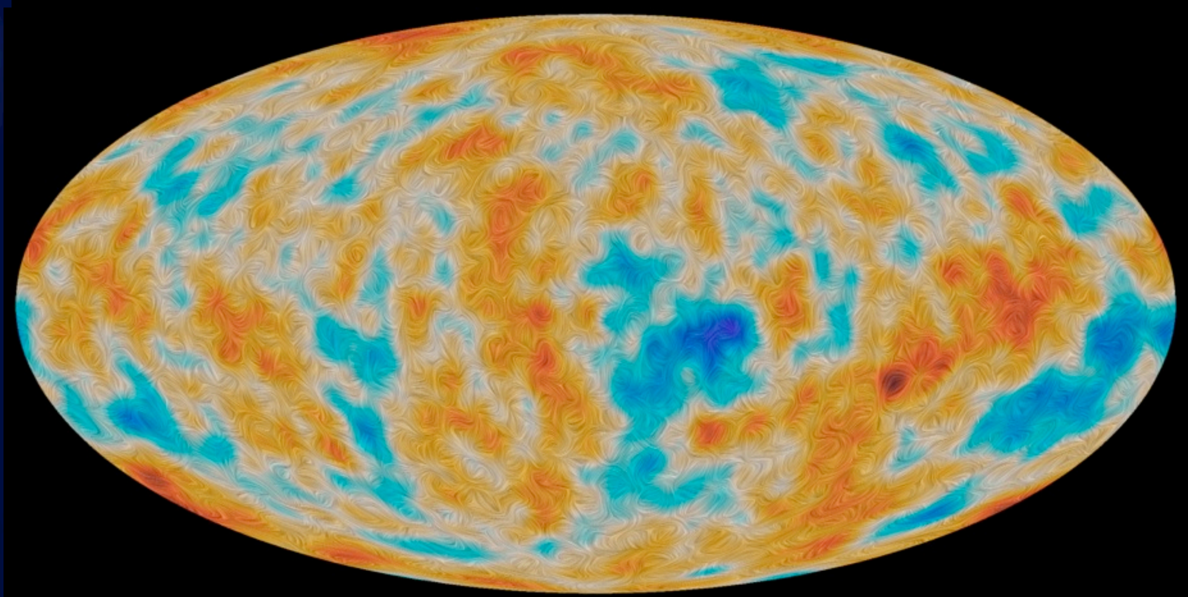

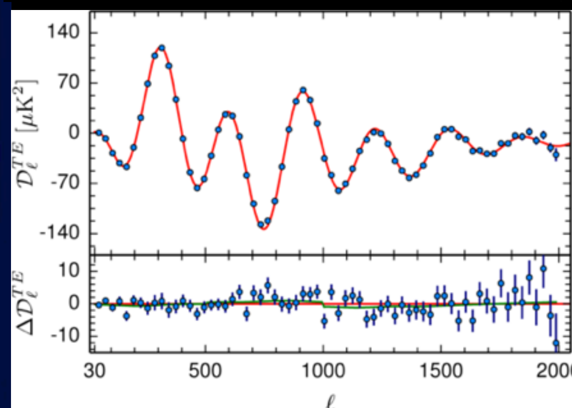
140
70
0
-70
-140
$\mathcal{D}_\ell^{TE}$ [μK^2]
10
0
-10
$\Delta\mathcal{D}_\ell^{TE}$
30
500
1000
1500
2000
ℓ

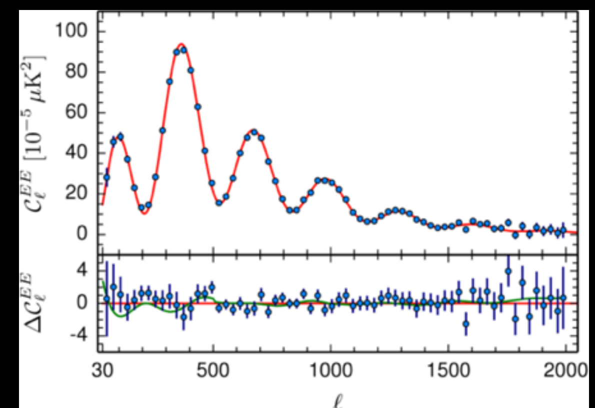
100
80
60
40
20
0
C_ℓ^{EE} [$10^{-5}\mu K^2$]
4
0
-4
ΔC_ℓ^{EE}
30
500
1000
1500
2000
ℓ

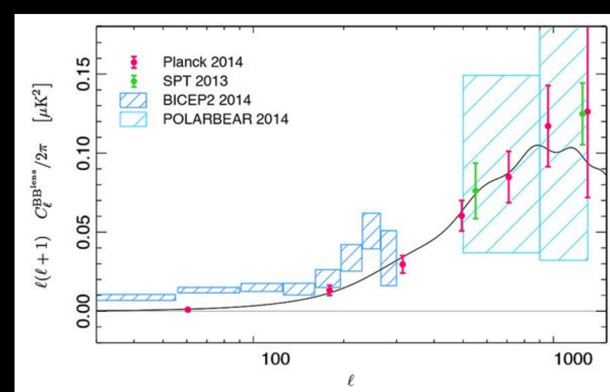
Planck 2014
SPT 2013
BICEP2 2014
POLARBEAR 2014
$\ell(\ell+1)\ C_\ell^{BB^{lens}}/2\pi$ [μK^2]
0.00
0.05
0.10
0.15
100
1000
ℓ

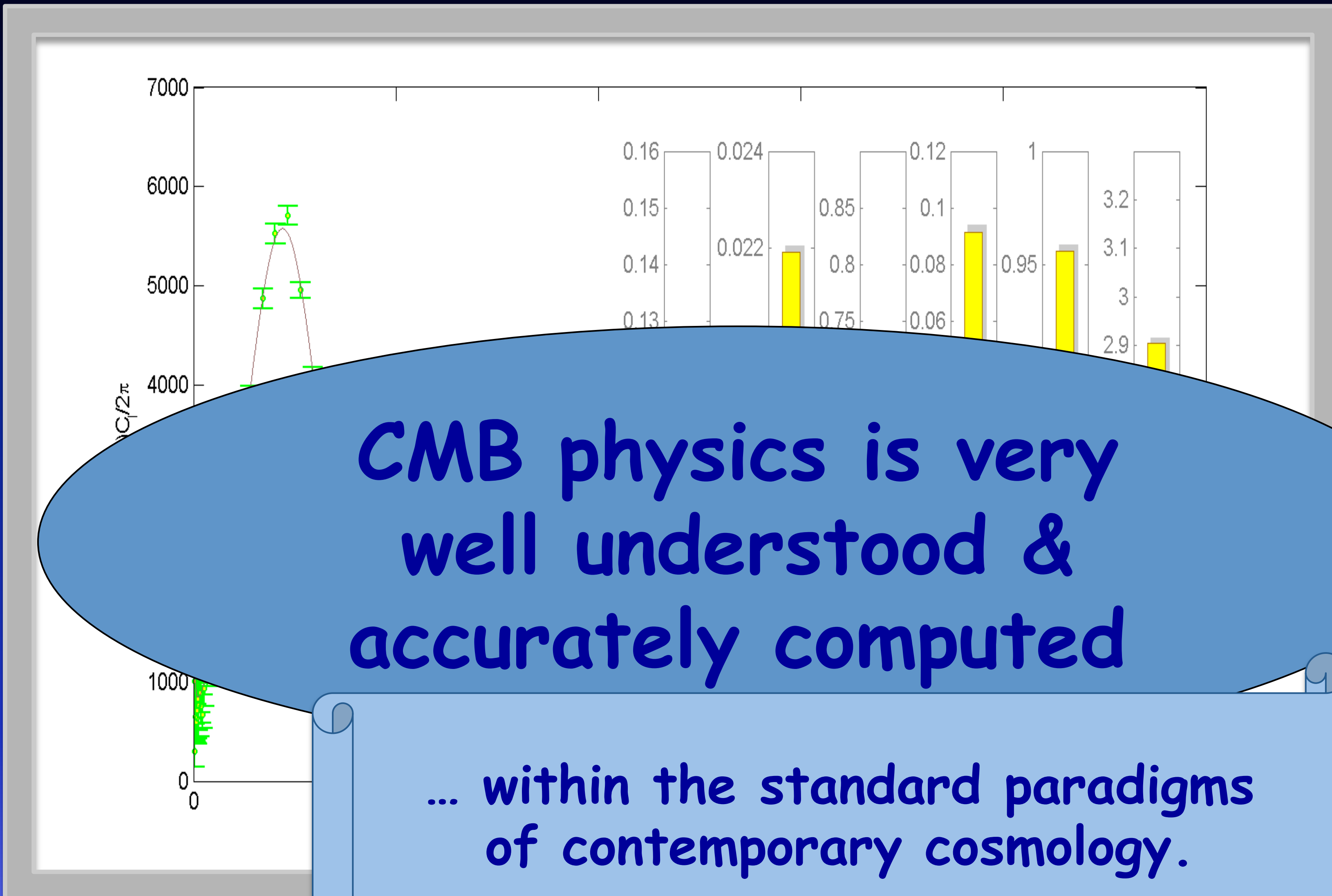

CMB physics is very well understood & accurately computed

… within the standard paradigms of contemporary cosmology.

CMB@IUCAA: CMBAns Boltzmann code by Santanu Das

Cosmological Parameters

6-Parameter ΛCDM

Parameter	*Planck* TT+lowP+lensing	
$\Omega_b h^2$	0.02226 ± 0.00023	1%
$\Omega_c h^2$	0.1186 ± 0.0020	1.7%
$100\theta_{MC}$	1.04103 ± 0.00046	0.04%
τ	[illegible]	
r_{drag}	[illegible]	
k_{eq}	0.01027 ± 0.00014	1.4%

'Standard' cosmological model:

***Flat, ΛCDM** with nearly*

Power Law (PL) primordial power spectrum

Paradigm of Statistical isotropy?

- a predicate of the Cosmological principle

Cosmic “Super–IMAX” theater

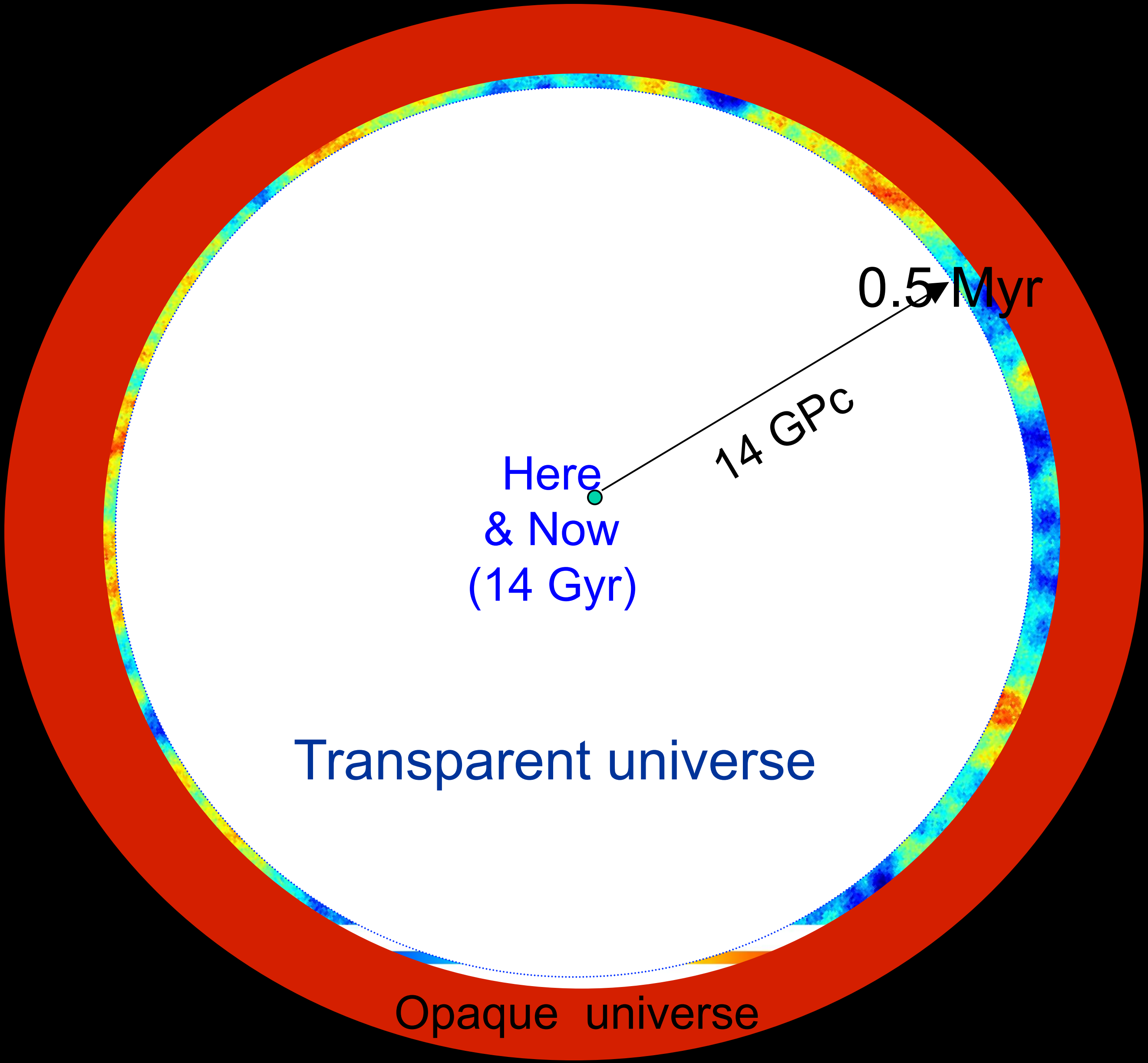

Cosmic Hemispherical Asymmetry

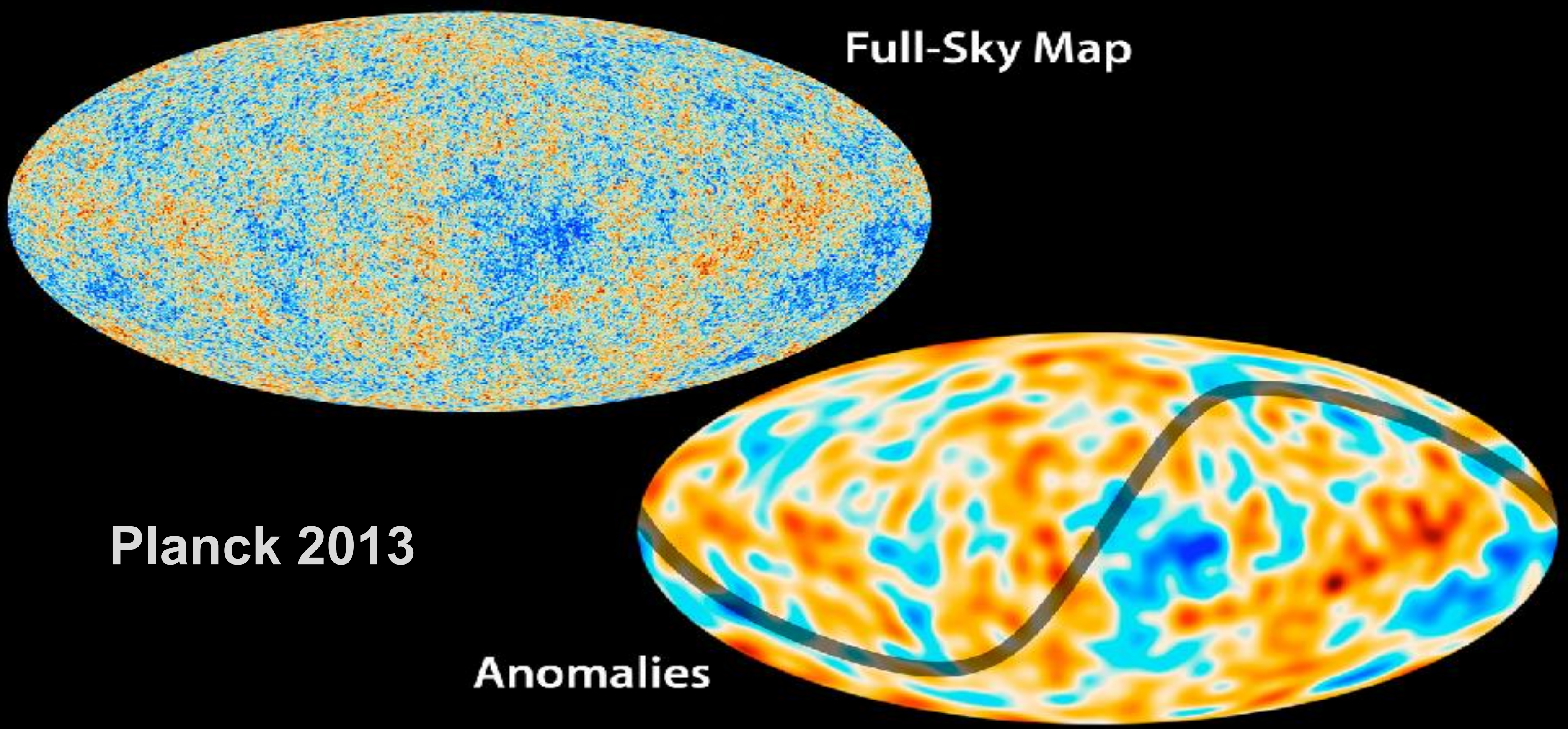

'Statistical Isotropy'

Statistical measures of the CMB sky fluctuations are invariant under rotations ➔ Homo. Random field on a sphere

$$\langle a_{lm} a^*_{l'm'} \rangle = C_l \; \delta_{ll'} \delta_{mm'}$$

Single index n:
(l,m) -> n

Diagonal Covariance matrix

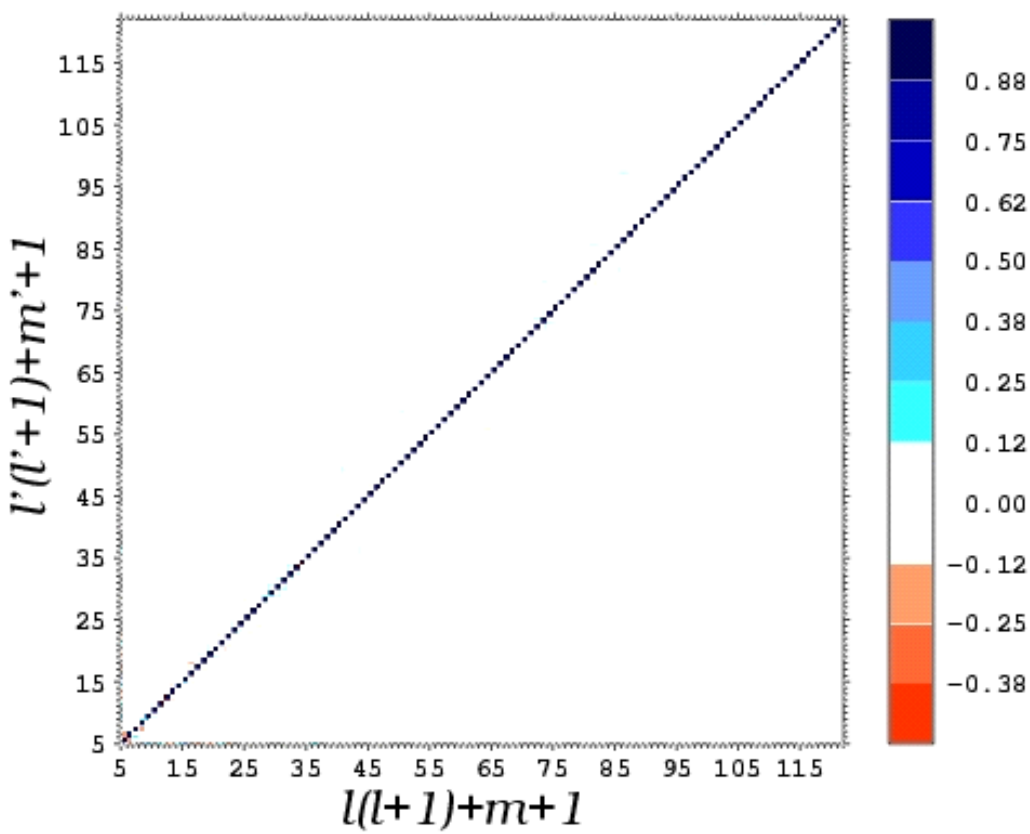

SI violation: $\left\langle a_{lm}\, a^{*}_{l'm'} \right\rangle \neq C_l\, \delta_{ll'} \delta_{mm'}$

Mild breakdown

$$\frac{\left\langle a_{lm} a^{*}_{l'm'} \right\rangle}{\sqrt{\left\langle a_{l'm'} a^{*}_{l'm'} \right\rangle \left\langle a_{lm} a^{*}_{lm} \right\rangle}}$$

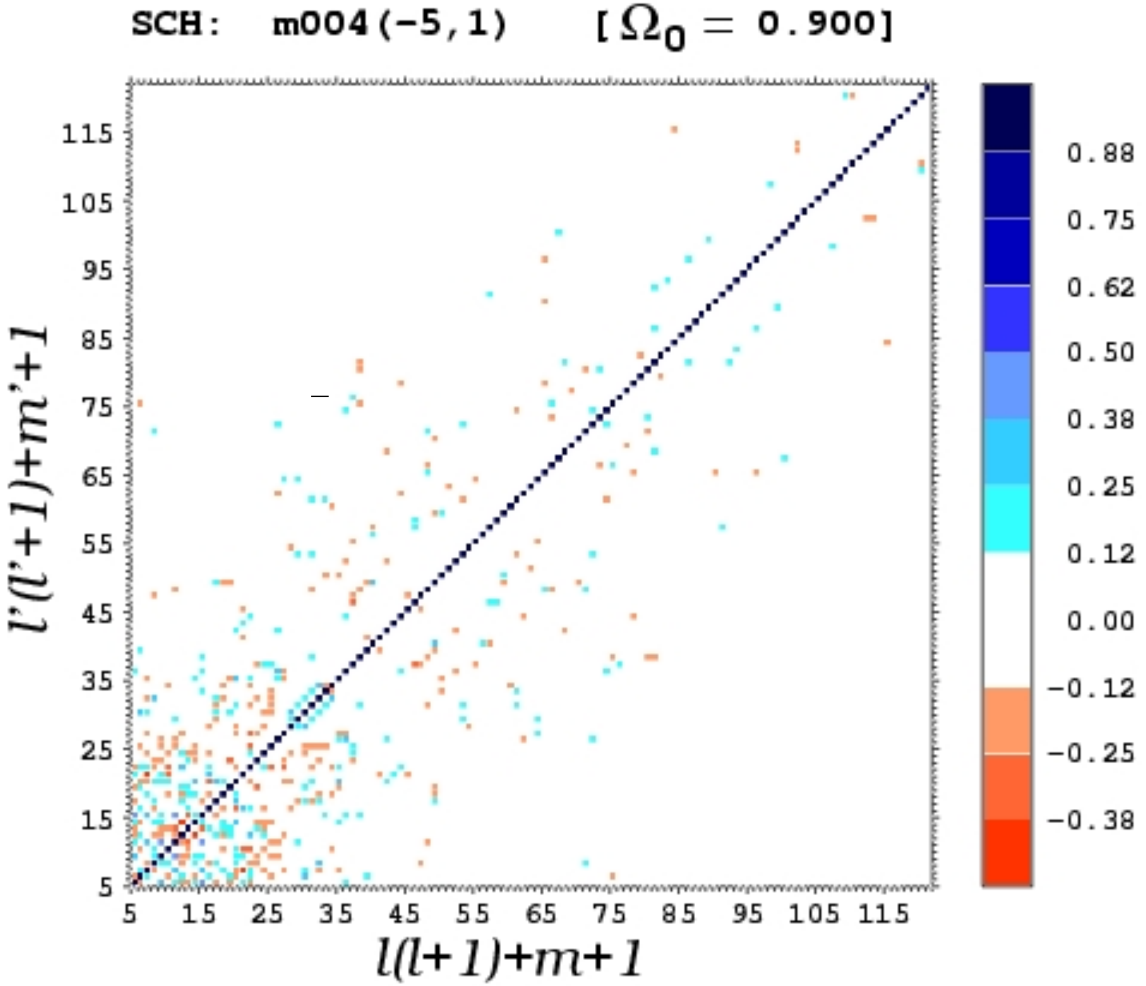

(Bond, Pogosyan & Souradeep 1998, 2002)

BipoSH Spectra : *Natural* generalization of C_ℓ

Amir Hajian & Souradeep 2003

$$\tilde{A}^{LM}_{l_1 l_2} = \sum_m \left\langle a^*_{l_1 m} a_{l_2 m+M} \right\rangle \; C^{LM}_{l_1 m l_2 m+M}$$

$A^{LM}_{l_1 l_2}$ → $\ddot{A}_{l_1 l_2}$: **Harmonic decomposition of map (temp, Pol)**

$A^{LM}_{l_1 l_2}$ → $A^{LM}_{\ddot{}}$: **Harmonic decomposition of non SI correlation.**

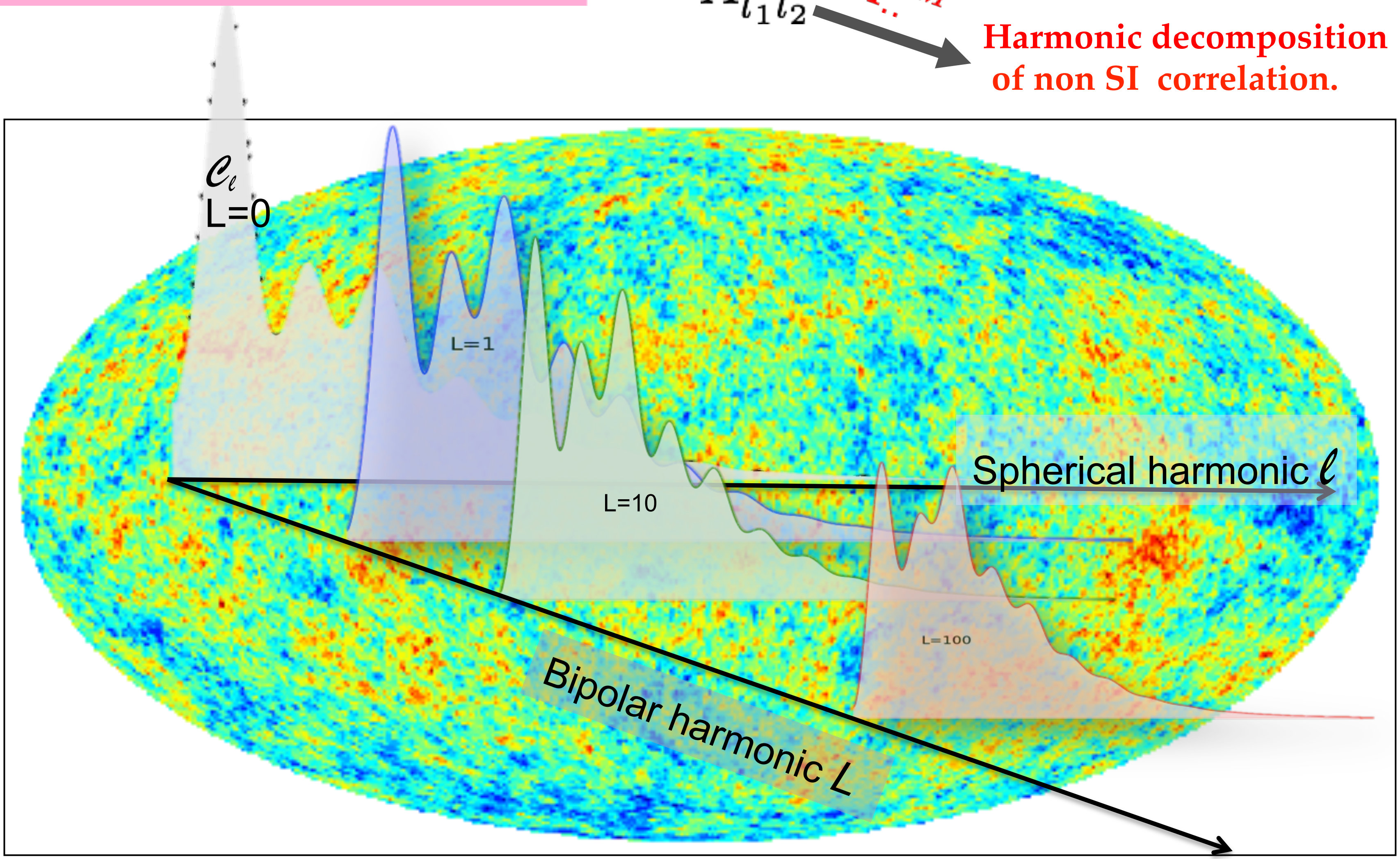

BipoSH Spectra : Natural generalization of C_ℓ

Bipolar Spherical Harmonic representation

Amir Hajian & Souradeep 2003

$$C(n_1 \bullet n_2) = \sum \frac{2l+1}{4\pi} C_l P_l(n_1 \bullet n_2)$$

$$C_\ell = \langle a_{\ell m} a^*_{\ell m} \rangle$$

$$C(\hat{n}_1, \hat{n}_2) = \sum_{l_1 l_2 LM} A^{LM}_{l_1 l_2} \{Y_{l_1}(\hat{n}_1) \otimes Y_{l_2}(\hat{n}_2)\}_{LM}$$

Bipolar spherical harmonics.

BipoSH
Coefficients

$$A^{LM}_{l_1 l_2} = \sum_m \langle a^*_{l_1 m} a^{\text{T, E, B,..}}_{l_2 m+M} \rangle \; C^{LM}_{l_1 m_1 l_2 m_+ M}$$

Linear combination of off-diagonal elements
BipoSH provide complete representation of SH space correlation matrix

Beyond C_l : *Patterns in CMB*

Sources of SI violation:

- Global topology
- Global anisotropy/rotation
- Breakdown of global symmetries, Magnetic field,…
- **Doppler boost:** Local motion *wrt* CMB
- **Weak Lensing**: Scalar (LSS) & tensor (GW)

Observational artifacts:

- Foreground residuals
- Inhomogeneous noise, coverage
- **Non-circular beam response function**

BipoSH spectra measurements

WMAP-7 : Bennet et al. 2010

$$\frac{A^{(+)LM}_{l_1 l_2}}{C^{L0}_{l0l'0}}$$

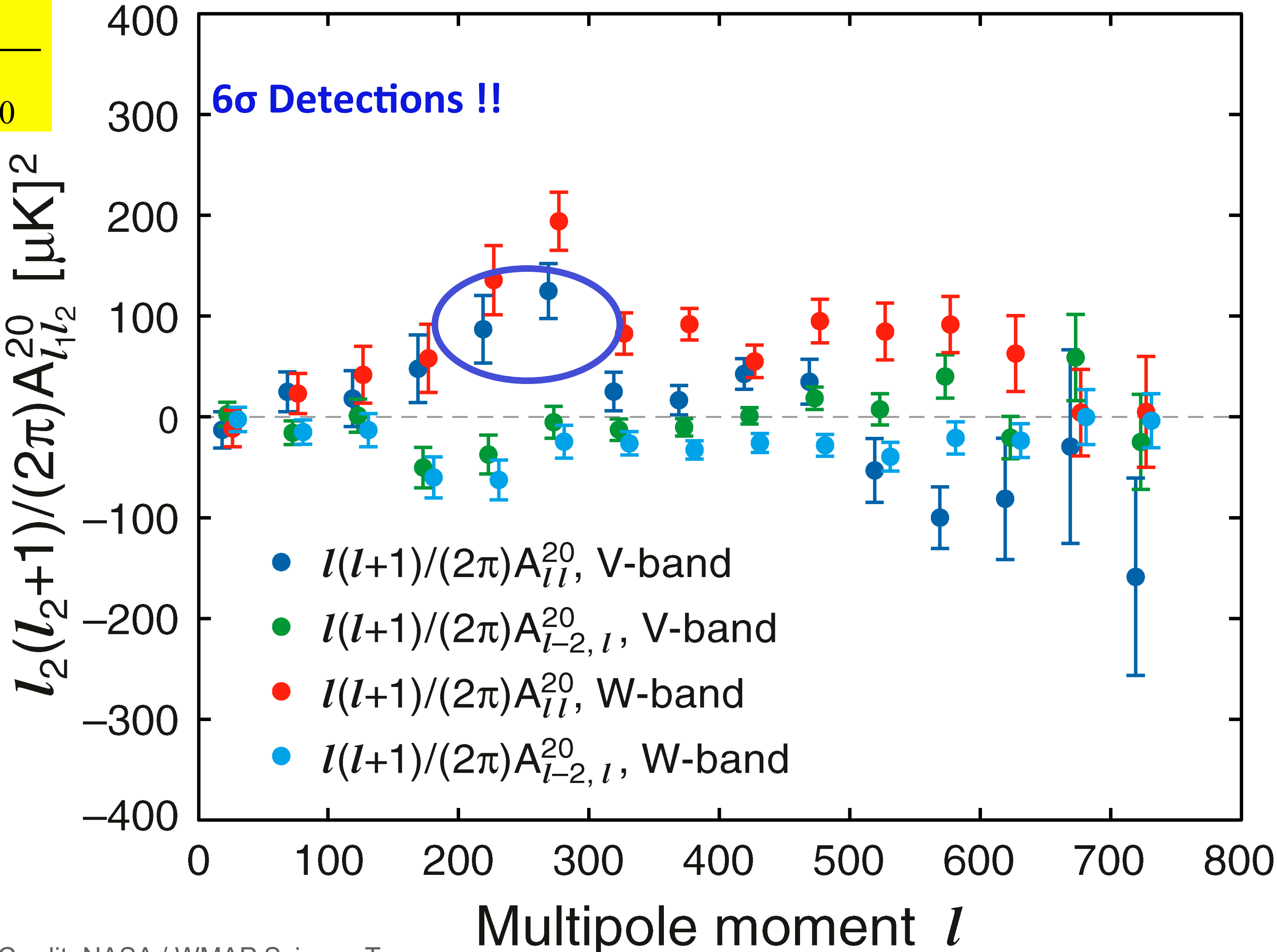

Image Credit: NASA / WMAP Science Team

WMAP-7 beams

(Nidhi Joshi, Santanu Das, Aditya Rotti, Sanjit Mitra, TS : A&A 2016)

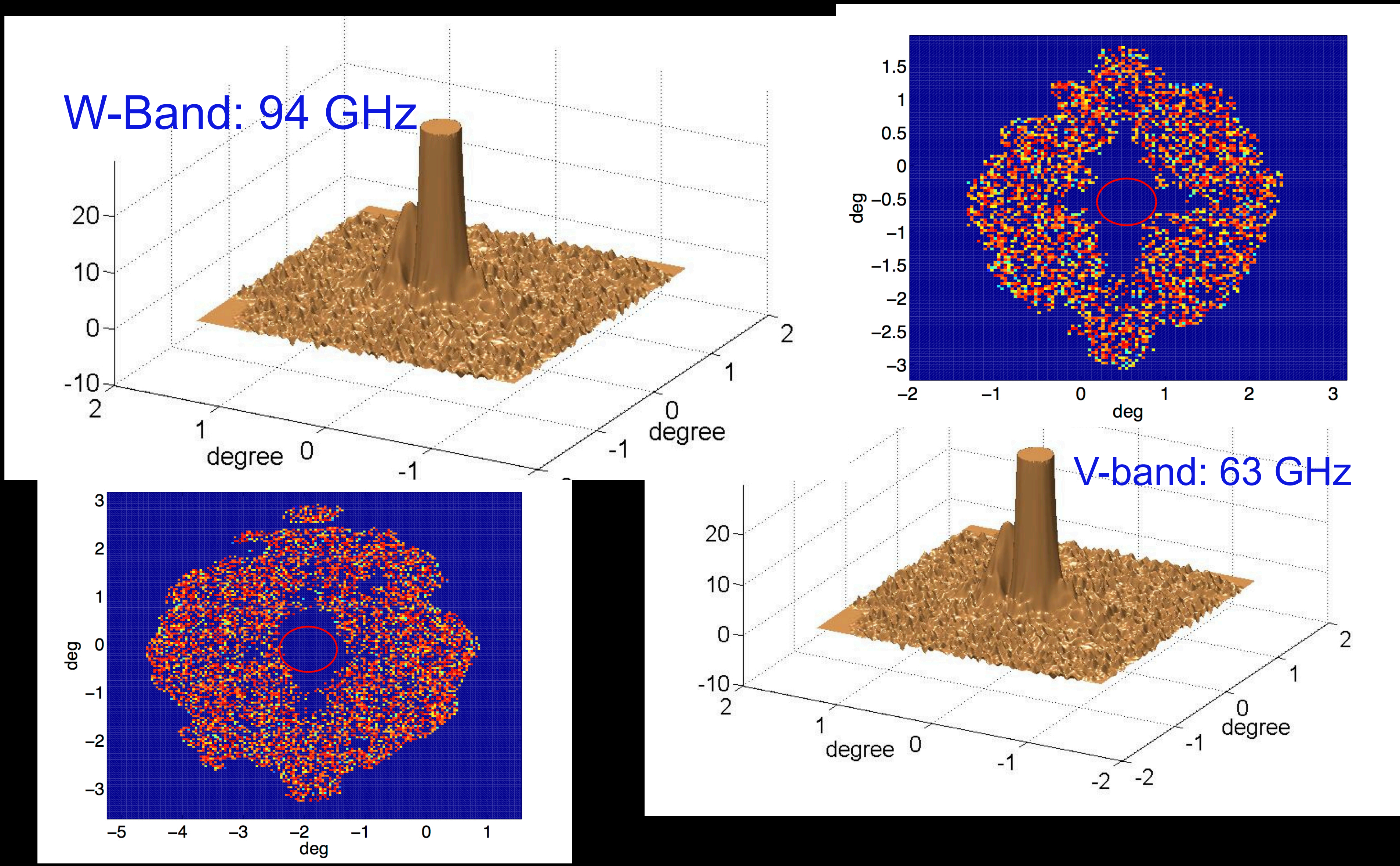

Full Num. WMAP-beam +Scan

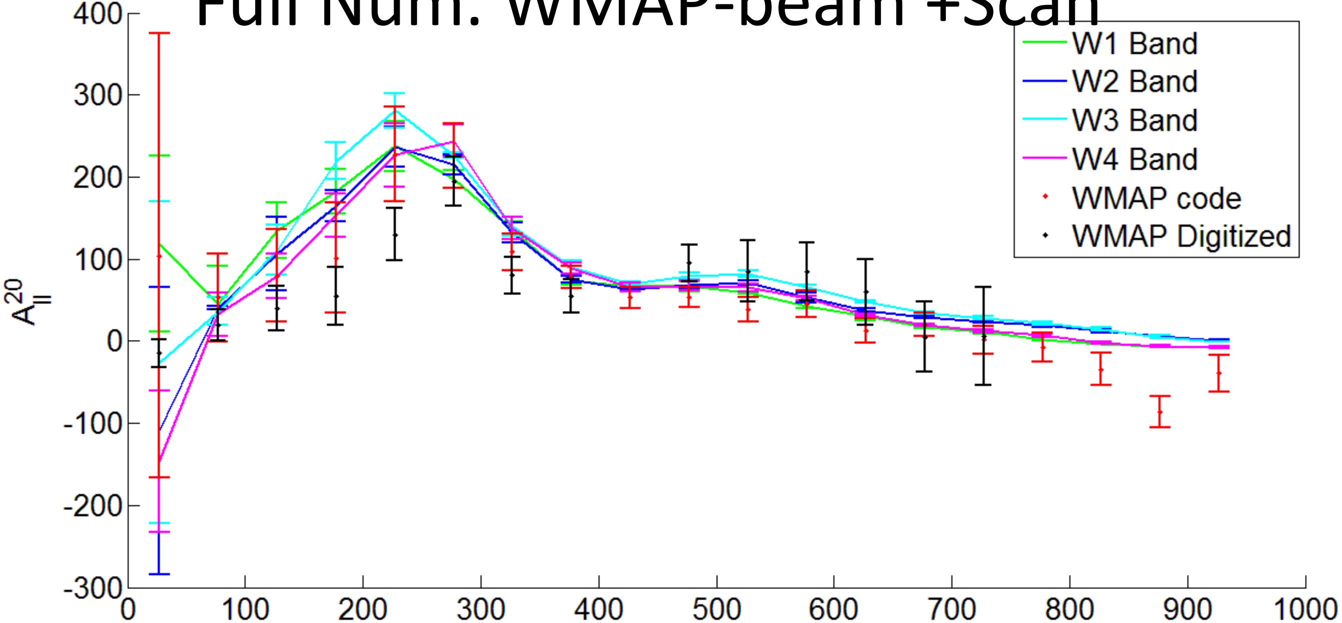

(Nidhi Joshi, Santanu Das, Aditya Rotti, Sanjit Mitra, TS : A&A 2016)

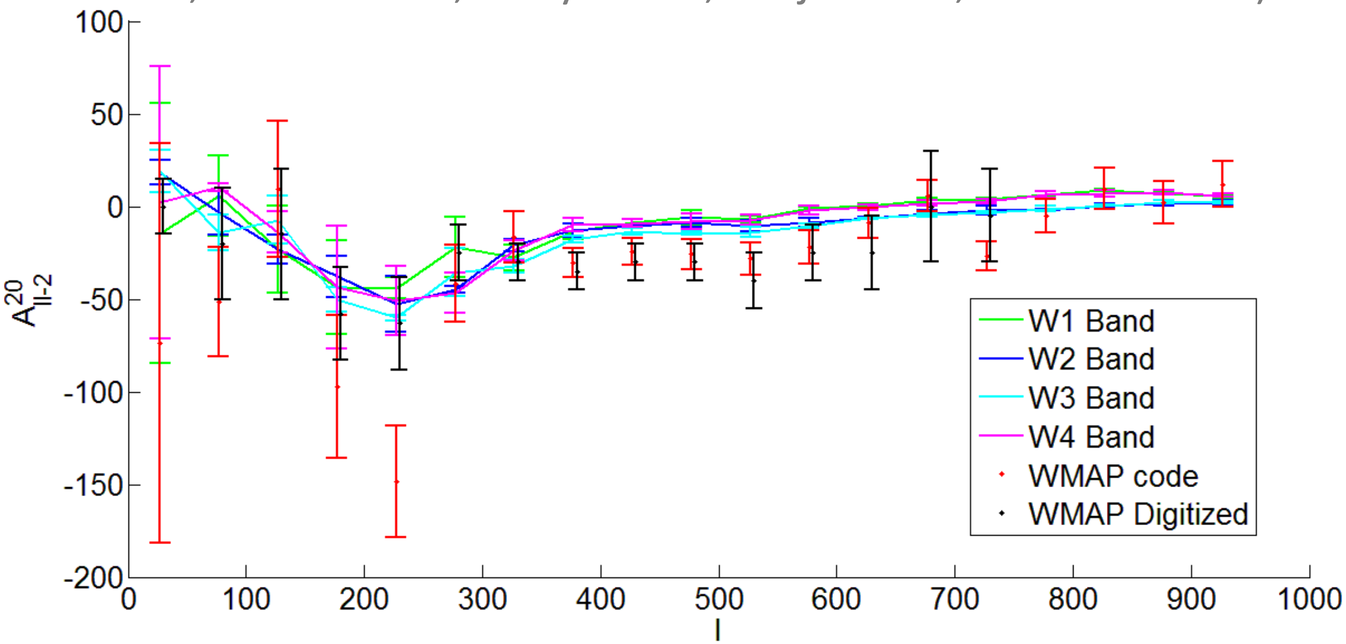

Weak Lensing

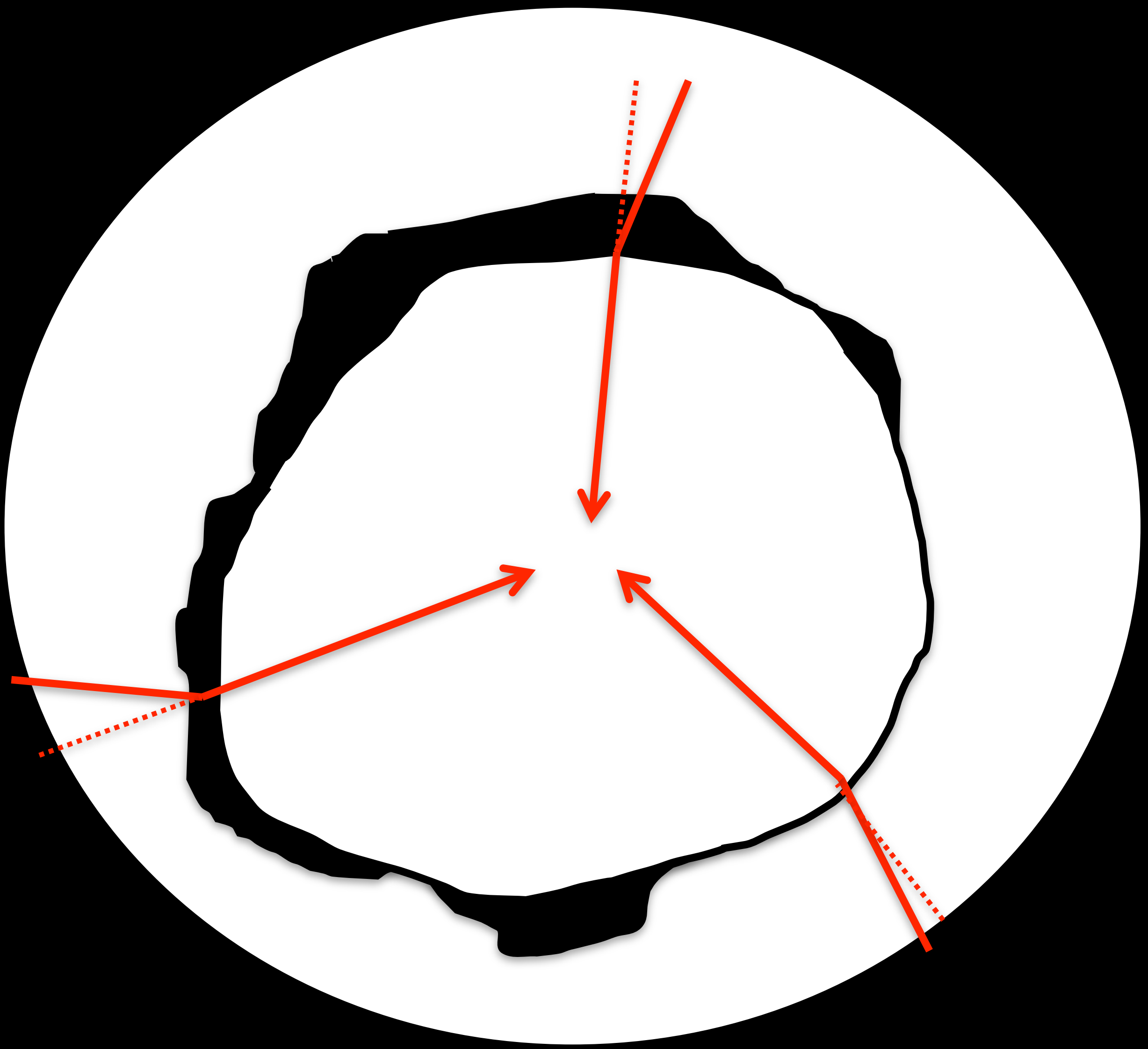

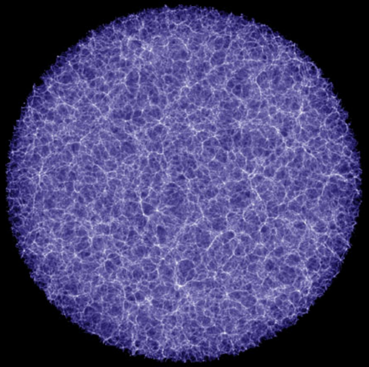

SI violation : Deflection field

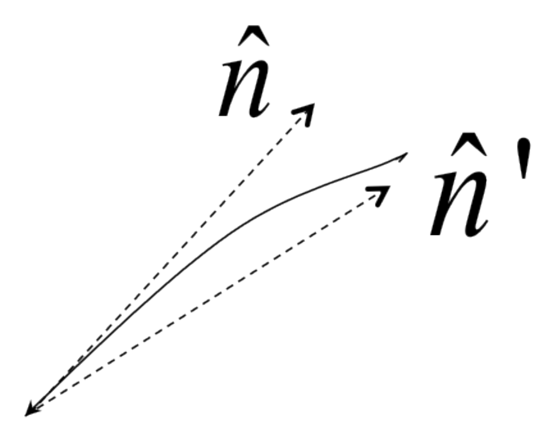

$$T(\hat{n}') = T(\hat{n} + \vec{\Theta}) = T(\hat{n}) + \vec{\Theta} \bullet \vec{\nabla} T(\hat{n})$$

$$\vec{\Theta} = \vec{\nabla}\phi(\hat{n}) + \vec{\nabla} \times \Omega(\hat{n})$$

$$= \nabla_i \phi(\hat{n}) + \varepsilon_{ij} \nabla_j \Omega(\hat{n})$$

Gradient Curl

WL:scalar WL: tensor/GW

Deflection field: Even & Odd parity BipoSH

Book, Kamionkowski & Souradeep, PRD 2012

$$A_{ll'}^{(+)LM} = \phi_{LM}\left[\frac{C_l G^L_{l'l}}{\sqrt{l'(l'+1)}} + \frac{C_{l'} G^L_{ll'}}{\sqrt{l(l+1)}}\right]$$

WL: scalar

$$A_{l_2 l_1}^{(-)LM} = i\Omega_{LM}\left[\frac{C_l G^L_{l'l}}{\sqrt{l'(l'+1)}} - \frac{C_{l'} G^L_{ll'}}{\sqrt{l(l+1)}}\right]$$

WL: tensor

BipoSH: Recovery of WL power spectrum

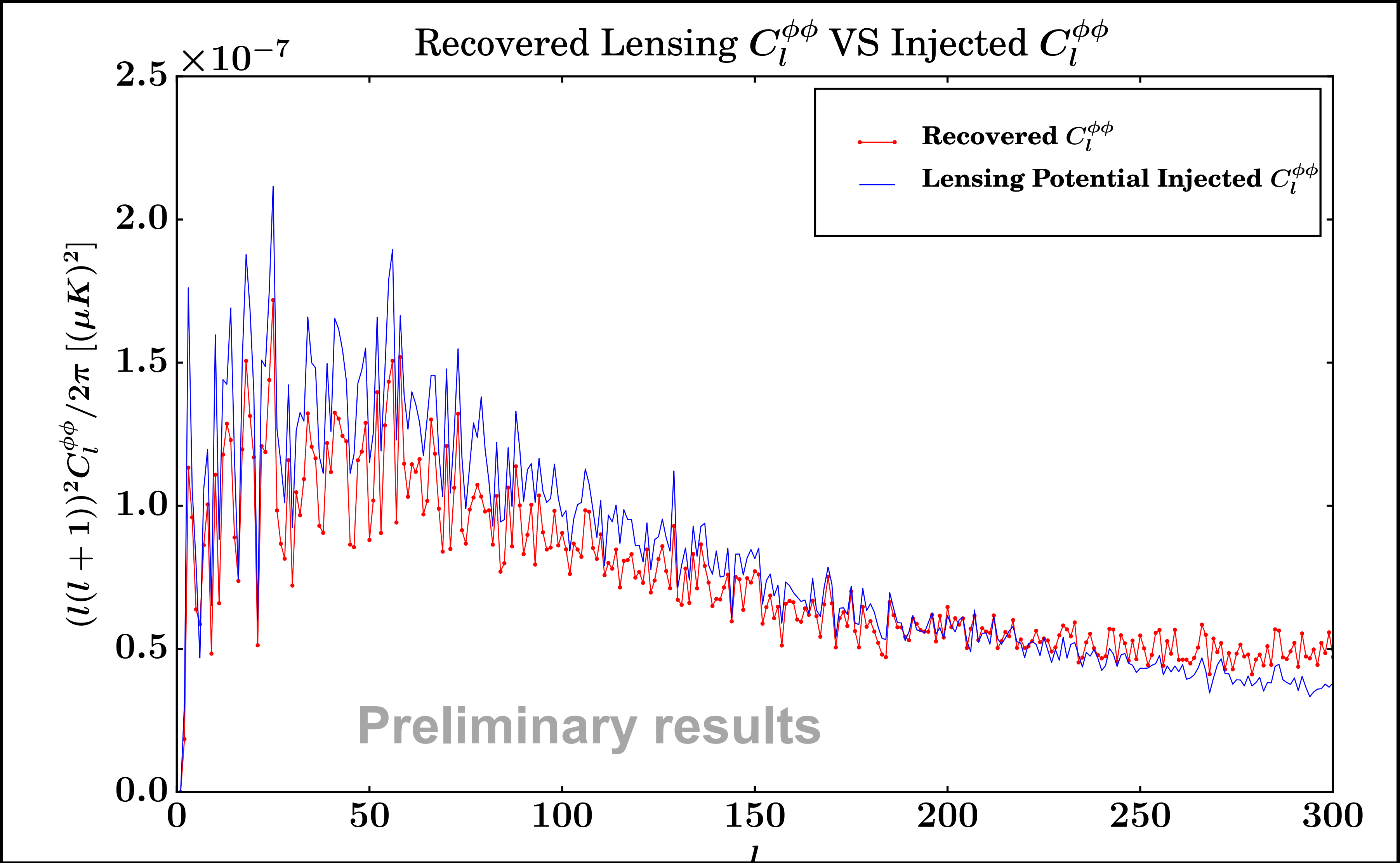

Statistical Isotropy violation in Reionization ?

- First brightest objects were formed at redshift $z \approx 30$ and start reionizing the surrounding medium. The universe becomes fully reionized by $z \approx 6$.
- Likely brightest objects were not formed isotropically. They reionize nearby regions earlier compared to the regions far away → **anisotropic reionization.**

$$\widetilde{T}(n) = T_0 + \triangle T e^{-\tau(n)}$$

$$(Q \pm iU)(\hat{\mathbf{n}}) = e^{-\tau(\hat{\mathbf{n}})} (Q \pm iU)^{(\mathrm{rec})}(\hat{\mathbf{n}})$$

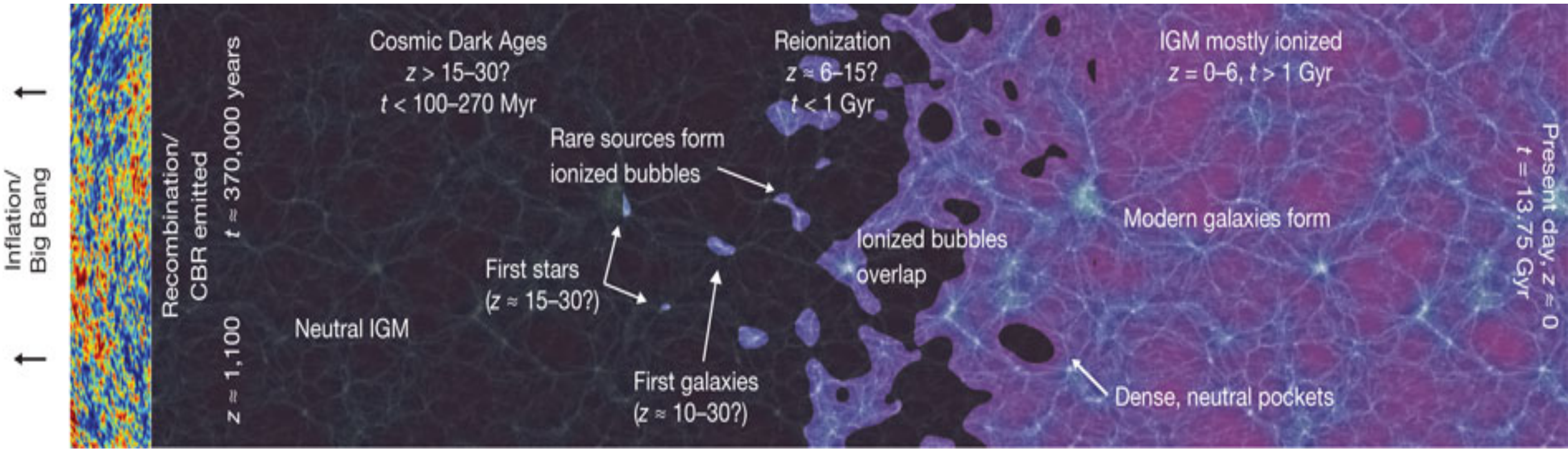

Reconstruction Noise

$$\tau(\hat{n}) = \bar{\tau} + \sum_{L>0} \Delta\tau_{LM}\ Y_{LM}(\hat{n})$$

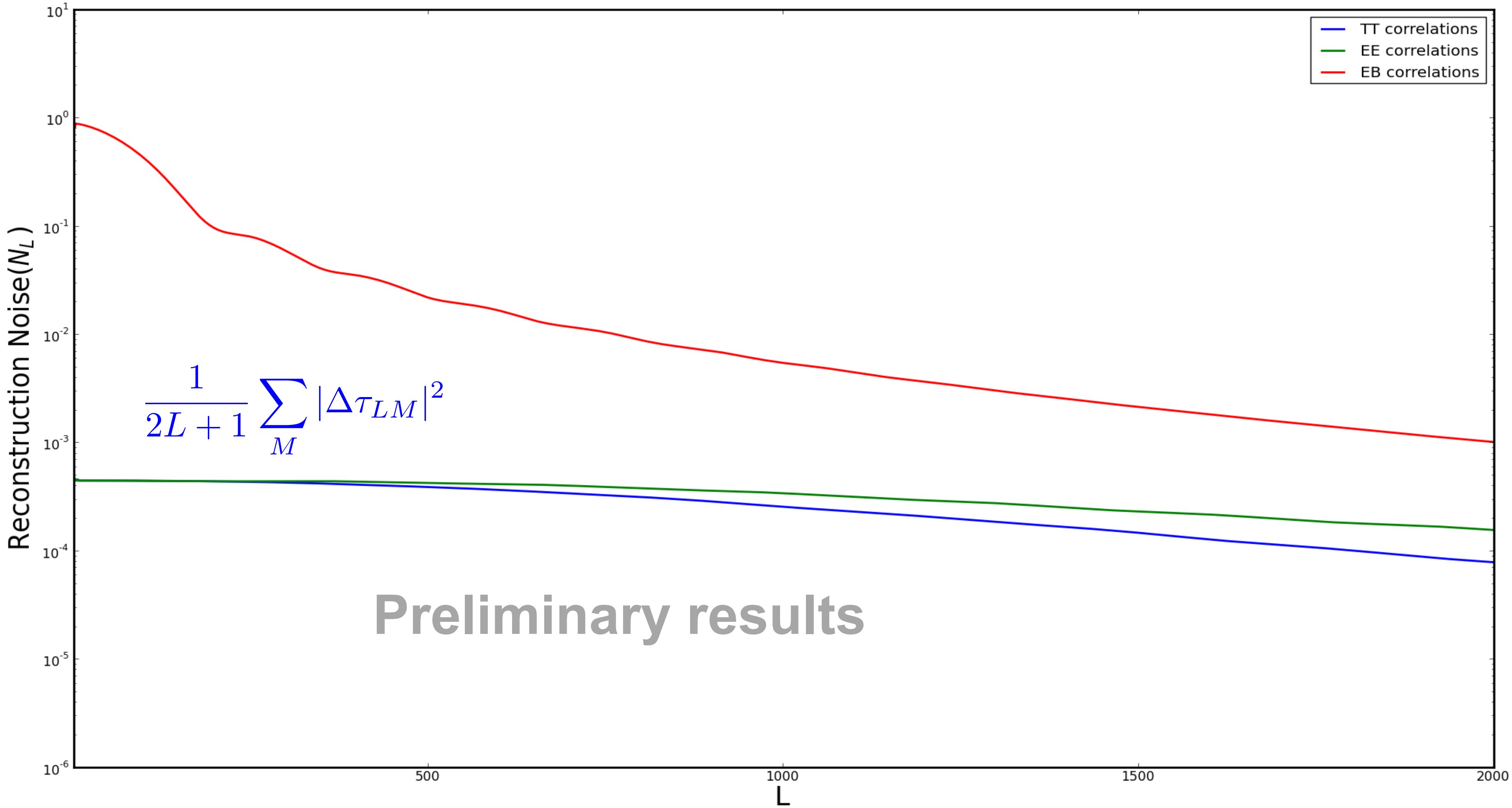

CMB fluctuations in a moving reference frame

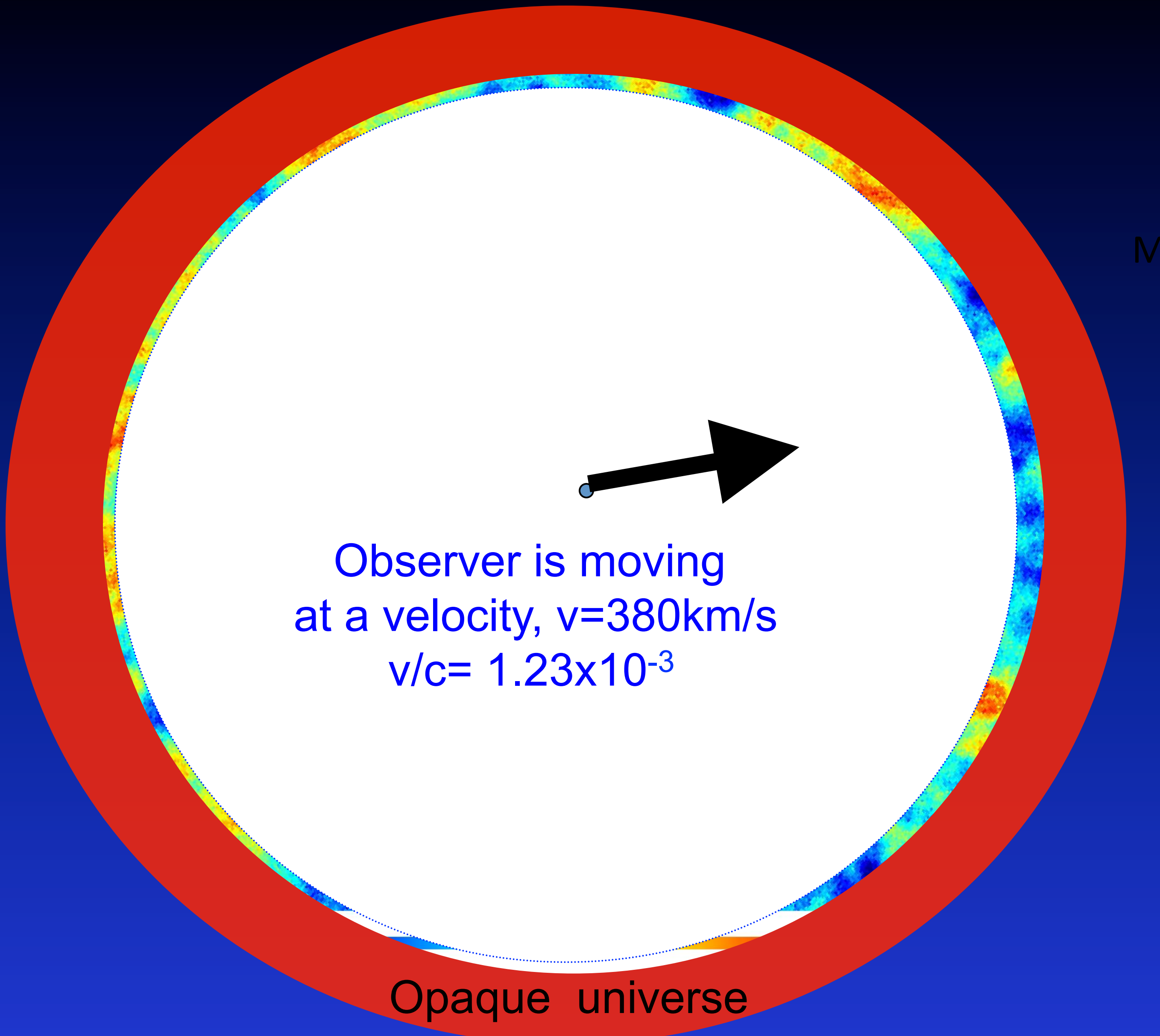

SI violation Doppler boost: BipoSH

Planck 2015 XVI: Isotropy & Statistics

Map	$\|\beta\| \times 10^{-3}$	Direction (l, b) [°]
SEVEM-100	1.24 ± 0.66	$(277, 40) \pm 50$
SEVEM-143	1.35 ± 0.56	$(264, 39) \pm 39$
SEVEM-217	1.28 ± 0.45	$(257, 42) \pm 32$

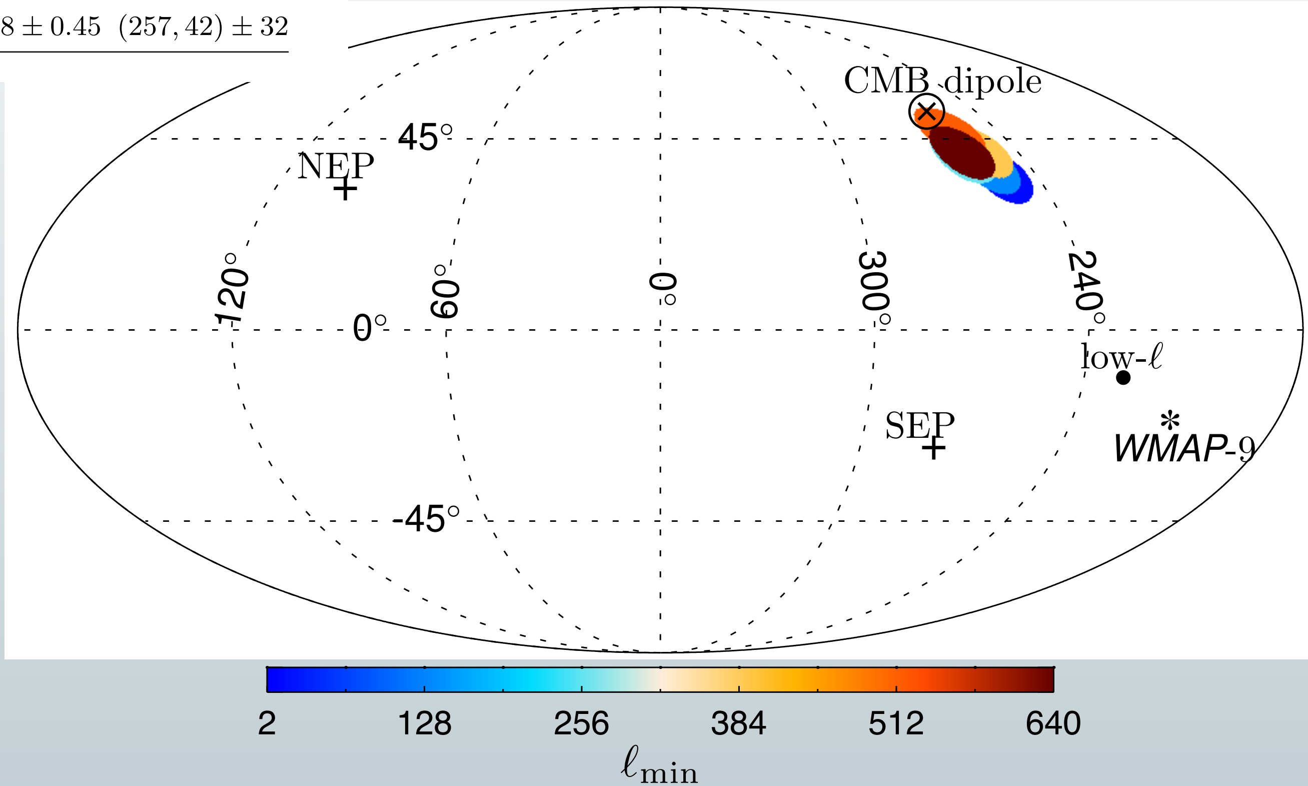

Fig. 34. *Top:* Amplitude $|\beta|$ of the Doppler boost from the SEVEM-100, SEVEM-143, and SEVEM-217 maps for different multipole bins determined using a BipoSH analysis. The maximum

Cosmic Hemispherical Asymmetry

planck

esa

ESA | SCIENCE & TECHNOLOGY | PLANCK

Missions
- Show All Missions

Mission Home
- Summary
- Fact Sheet
- Objectives

Participants
- Mission Team
- Industrial Team

Science Results
- Planck's cosmology
- Cosmic structure
- Through the Milky Way

Spacecraft
- Spacecraft
- 3D Model
- Instruments
- Cooling system

Mission Operations

HEMISPHERIC ASYMMETRY AND COLD SPOT IN THE COSMIC MICROWAVE BACKGROUND

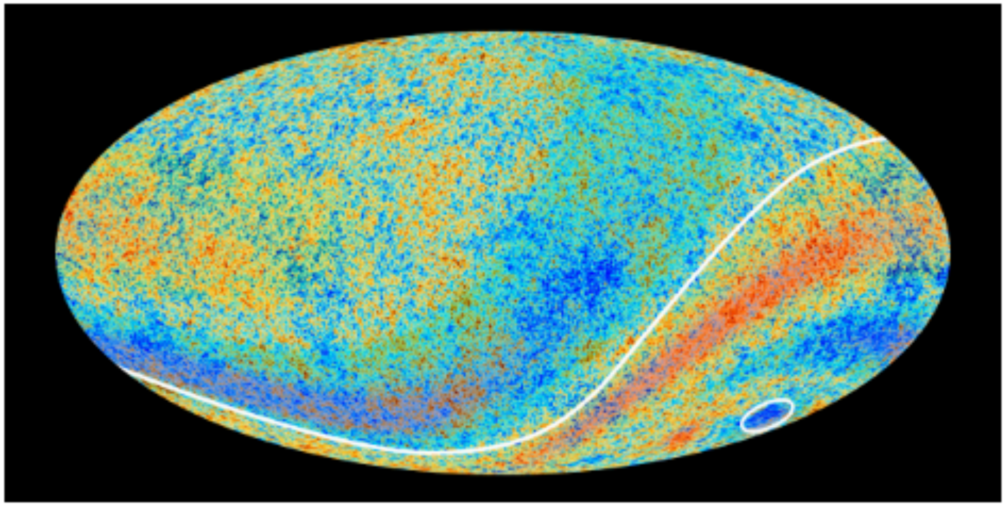

Date: 21 March 2013
Satellite: Planck

Two Cosmic Microwave Background anomalous features hinted at by Planck's predecessor, NASA's Wilkinson Microwave Anisotropy Probe (WMAP), are confirmed in the new high precision data from Planck. One is an asymmetry in the average temperatures on opposite hemispheres of the sky (indicated by the curved line), with slightly higher average temperatures in the southern ecliptic

Search here

5-Oct-2016 17:02 UT

Shortcut URL
http://sci.esa.int/jump.cfm?oid=51559

Also Available As
JPG 3410 × 1705
4.6 MB

Related Links
- Planck cosmology results 2013
- Planck Legacy Archive

See Also
- Simple but challenging: the Universe according to Planck

Cosmic Hemispherical Asymmetry

Need non-SI simulations to perform statistical analysis

Salient features of
…Hemispherical Asymmet…

…ed a…
…atio…

Implications of the asymmetry on the derived cosmological parameters

Essential aspects to understand the "Pesky CHA"

➢ NON-ALIGNED: Directi… b = −18◦) ± 30◦, which is not aligned with the Ga…

➢ACHROMATIC: similar signal … …ry is observed at three Planck frequencies (100, 143, 217 GHz). T… …e two features reduce the chance of its origin from some residual foregro…d contaminations.

To understand the origin of CHA

…e observed excess power is of …
…ular scales (l<70). Hence, the a…
…enon.

To find other cosmological probes to CHA

Modulation model of SI violation

$$\Delta T(\hat{n}) = [1 + M(\hat{n})]\Delta T^{\rm SI}(\hat{n})$$

M(n) : modulation field searched $M(\hat{n}) = \sum_{LM} m_{LM} Y_{LM}(\hat{n})$

Focus only on L=1 Dipole Modulation in 2014

$$\Delta T(\hat{n}) = [1 + A\ (\hat{p}.\hat{n})]\ \Delta T^{\rm SI}(\hat{n})$$

$$A = 1.5\sqrt{\frac{m_1}{\pi}}$$

$$m_1 = \frac{|m_{10}|^2 + |m_{11}|^2 + |m_{1-1}|^2}{3}$$

Dipole modulation

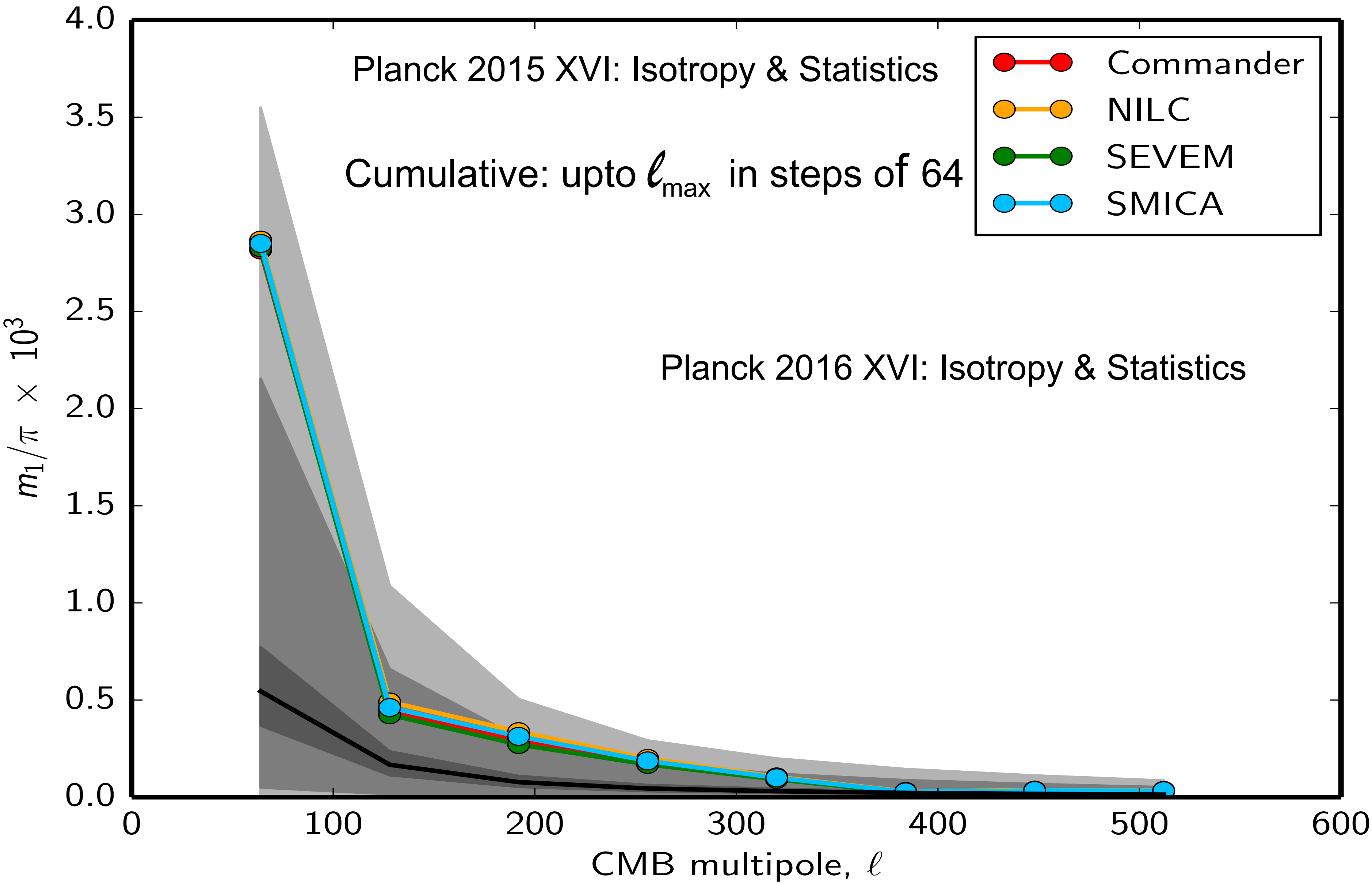

Dipole modulation : Frequency independence

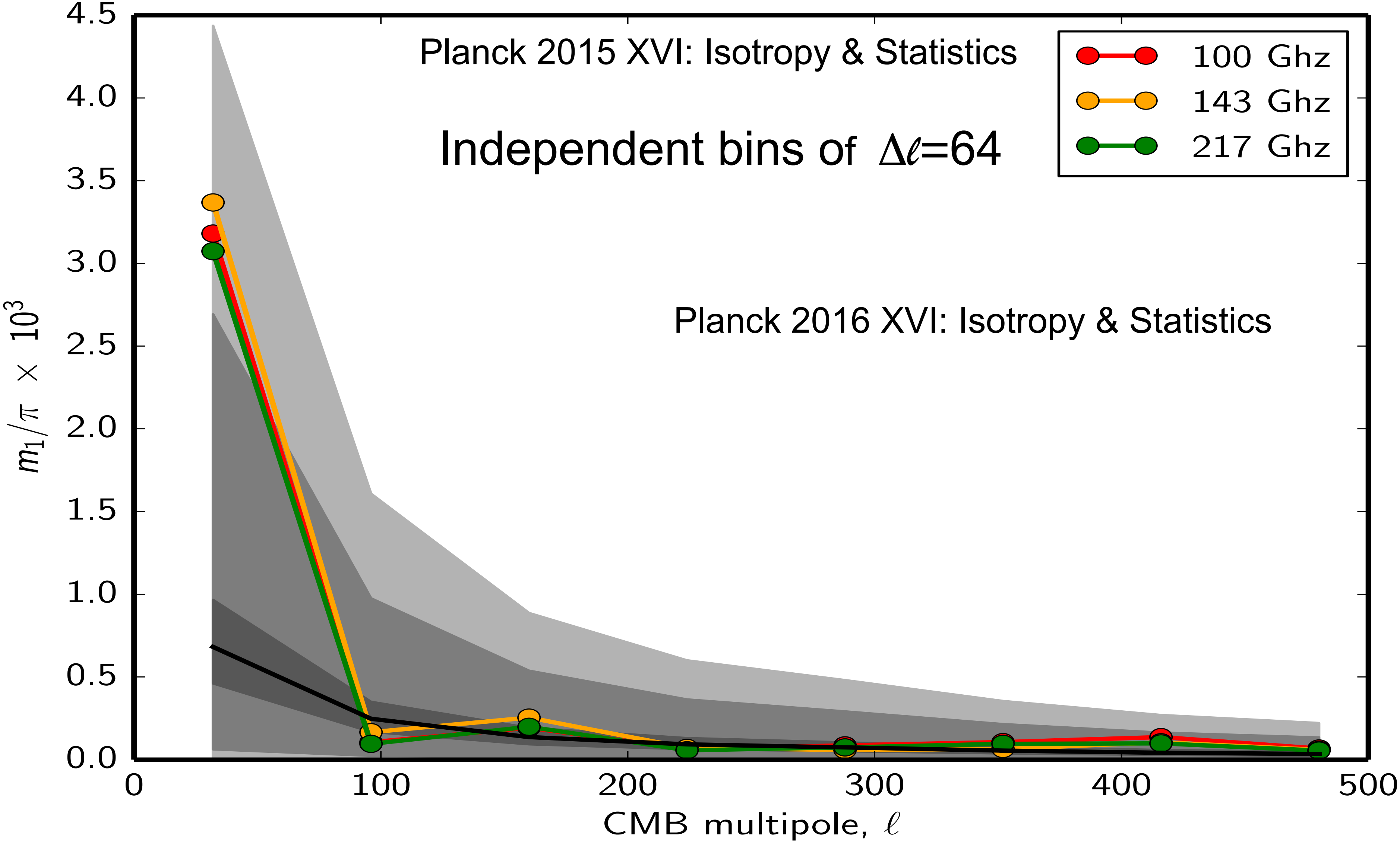

Dipole modulation: Scale Dependence

Planck 2016 SMICA

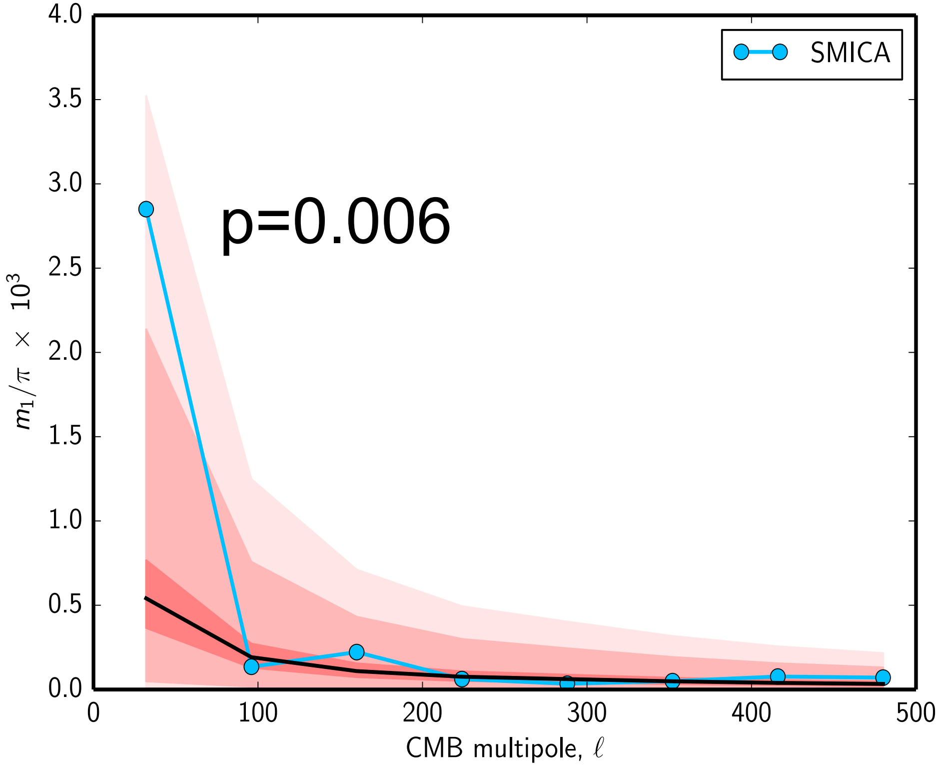

Planck 2014 SMICA

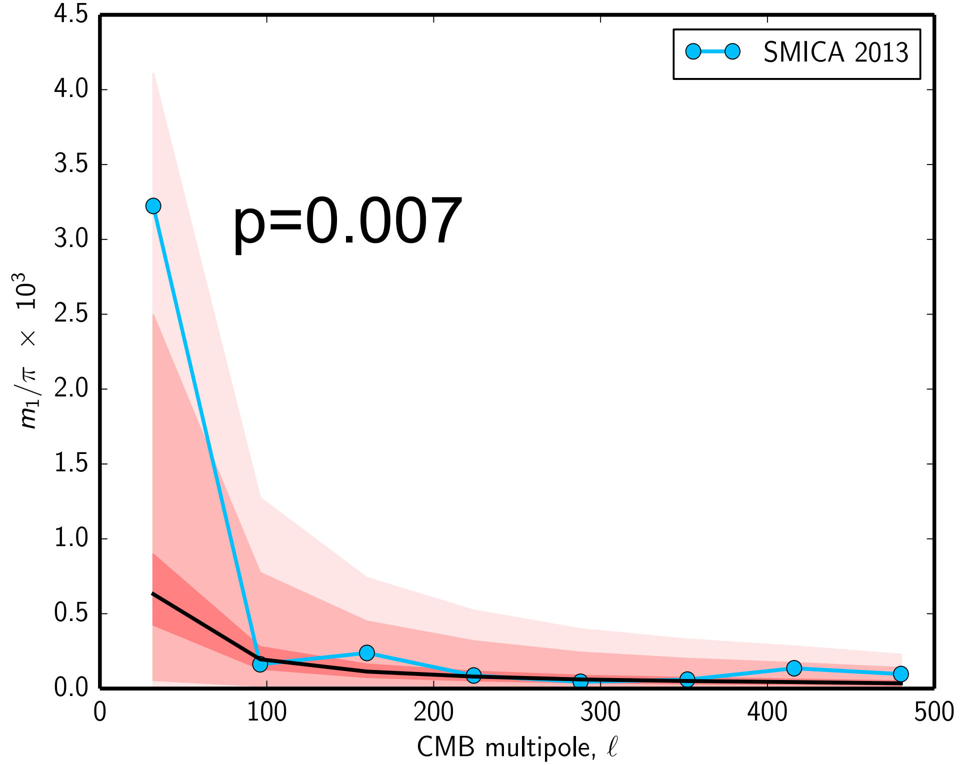

Hemispherical power asymmetry

Direction deduced from BipoSH Analysis

Planck 2015 XVI: Isotropy & Statistics

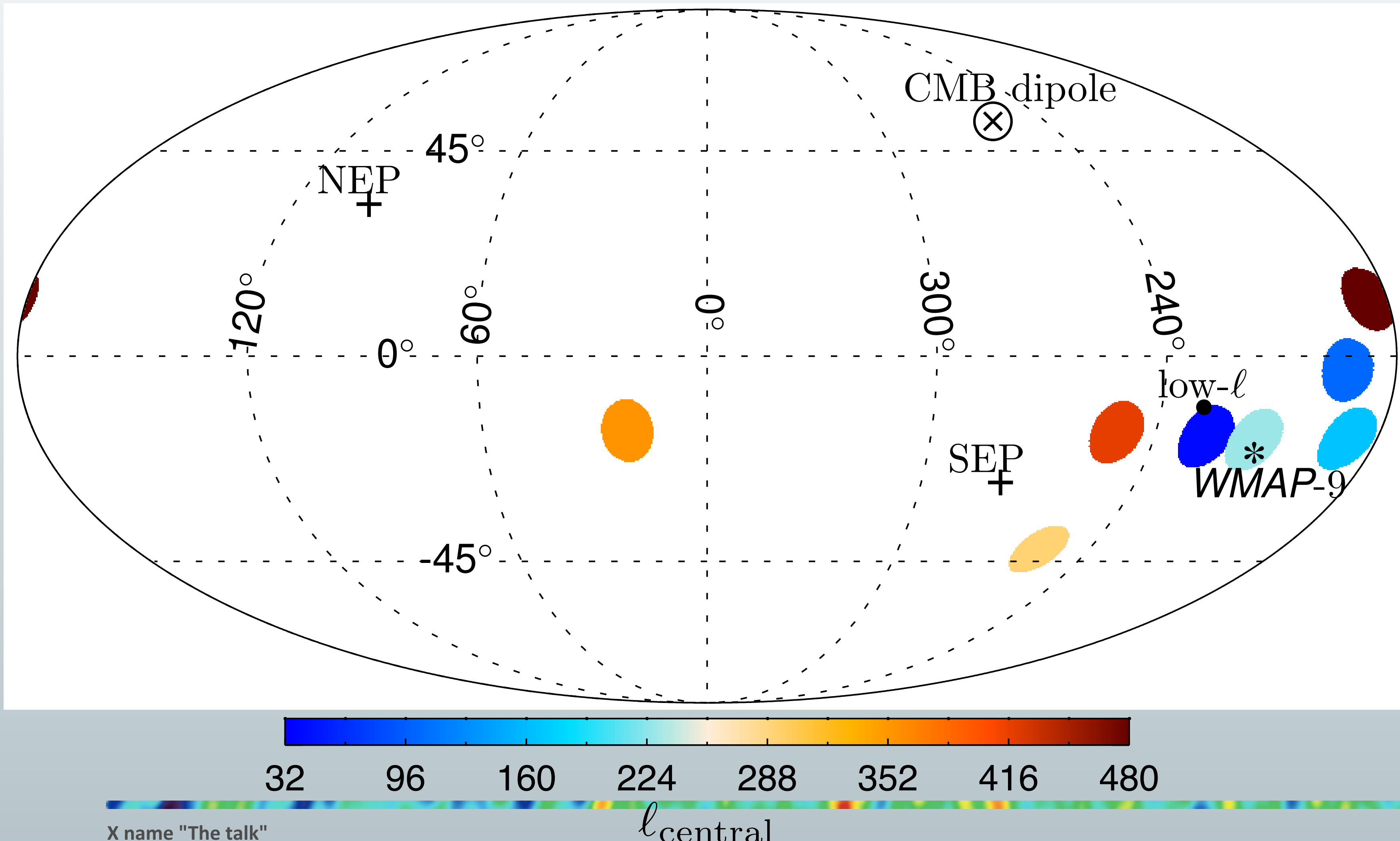

Planck CMB sky maps & spectra

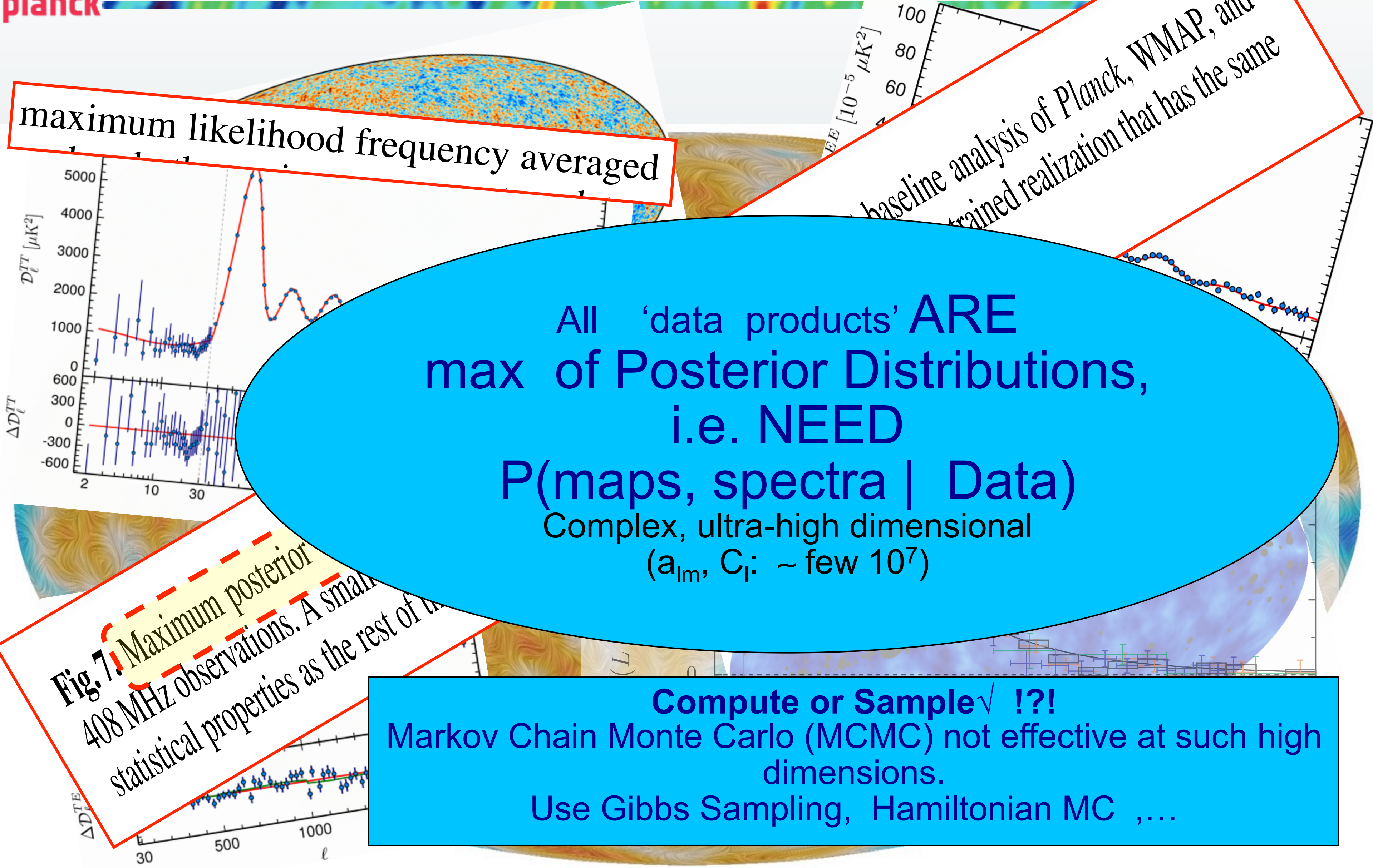

All ‘data products’ ARE
max of Posterior Distributions,
i.e. NEED
P(maps, spectra | Data)
Complex, ultra-high dimensional
(a_{lm}, C_l: ~ few 10^7)

Compute or Sample√ !?!
Markov Chain Monte Carlo (MCMC) not effective at such high dimensions.
Use Gibbs Sampling, Hamiltonian MC ,…

Probability distribution

$$P(\mathbf{S},\mathbf{a}|\mathbf{d}) = \frac{1}{\sqrt{|\mathbf{N}||\mathbf{S}|}(2\pi)^n} \exp -\frac{1}{2}\Big[(\mathbf{d}-\mathbf{a})^\dagger \mathbf{N}^{-1}(\mathbf{d}-\mathbf{a}) + \mathbf{a}^\dagger \mathbf{S}^{-1}\mathbf{a}\Big]$$

$$P(C_l, m_{10}, m_{11}, m_{1-1}|\mathbf{d}) = \frac{1}{\sqrt{|\mathbf{N}+\mathbf{S}|}(2\pi)^{n/2}} \exp -\frac{1}{2}\Big[\mathbf{d}^\dagger(\mathbf{S}+\mathbf{N})^{-1}\mathbf{d}\Big]$$

$\mathbf{S}(C_l, m_{10}, m_{11}, m_{1-1})$ - parameter dependence of covariance matrix

---

Under the assumption that the noise matrix is diagonal, if S + N has following form:

$$\mathbf{S}+\mathbf{N} = \mathbf{D} + m_{10}\mathbf{O_1}$$

D: Diagonal of the matrix S + N
O_1: Offdiagonal part of the matrix S without m_{10}

$$P(C_l, m_{10}|\mathbf{d}) = \frac{1}{\sqrt{|\mathbf{D}|}(2\pi)^{n/2}} \exp\Big[-\frac{1}{2}\mathbf{d}^\dagger\mathbf{D}^{-1}\mathbf{d}\Big] \exp\Big[-\frac{(m_{10}-\mu)^2}{2\sigma^2}\Big] \exp\Big[\frac{\mu^2}{2\sigma^2}\Big]$$

n is number of data points.

Conditional Mean:

$$\mu = \frac{d^\dagger D^{-1}O_1 D^{-1}d}{tr[(D^{-1}O_1)^2]}\Big[2\frac{d^\dagger(D^{-1}O_1)^2 D^{-1}d}{tr[(D^{-1}O_1)^2]} - 1\Big]^{-1}$$

Conditional variance:

$$\sigma^2 = \frac{2}{tr[(D^{-1}O_1)^2]}\Big[2\frac{d^\dagger(D^{-1}O_1)^2 D^{-1}d}{tr[(D^{-1}O_1)^2]} - 1\Big]^{-1}$$

Bayesian inference on the sphere beyond statistical isotropy

Santanu Das, B.Wandelt, TS JCAP 2015
(ArXiv: 1509.07137)

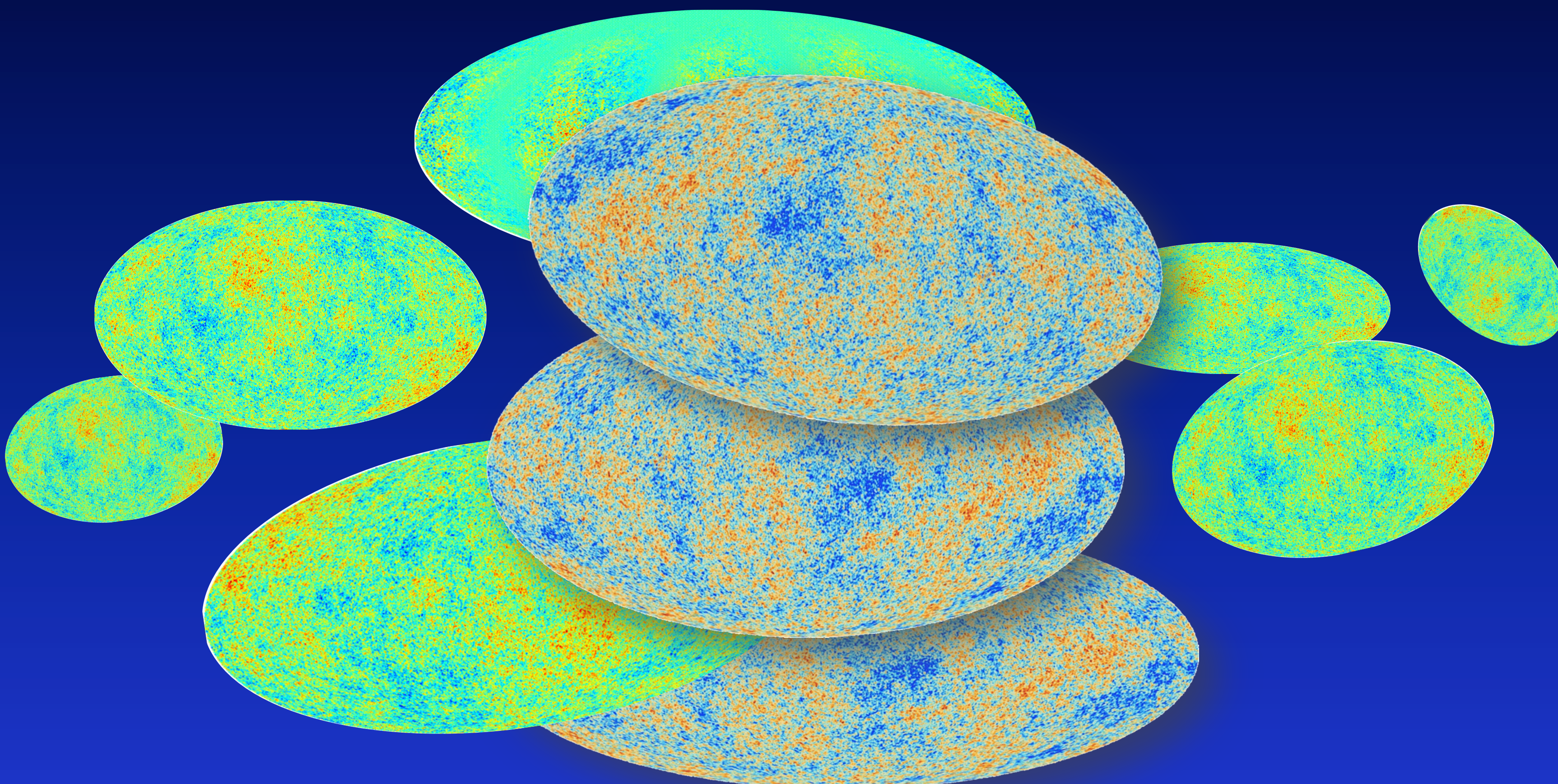

Observed Sky Temp | Original Sky Temp | Noise

Observed sky : $\tilde{T}(\gamma) = T(\gamma) + N(\gamma)$

Spherical Harmonics basis : $d_{lm} = a_{lm} + n_{lm}$

$$P(S_{lml'm'}|d_{lm}) \propto P(d_{lm}|a_{lm})P(a_{lm}|S_{lml'm'})P(S_{lml'm'})$$

$$= \frac{1}{\sqrt{|N_l|}} \exp\left[-\frac{1}{2}(d^*_{lm} - a^*_{lm})^T N_l^{-1} (d_{lm} - a_{lm})\right]$$

$$\times \frac{1}{\sqrt{|S_{lml'm'}|}} \exp\left(-\frac{1}{2} a^{*T}_{lm} S^{-1}_{lml'm'} a_{lm}\right)$$

We use **Hamiltonian Monte Carlo** method for sampling the Posterior

$\langle a_{lm} a^*_{l'm'} \rangle$

Test on Stat. Isotropic maps: $\mathcal{C}_\ell$

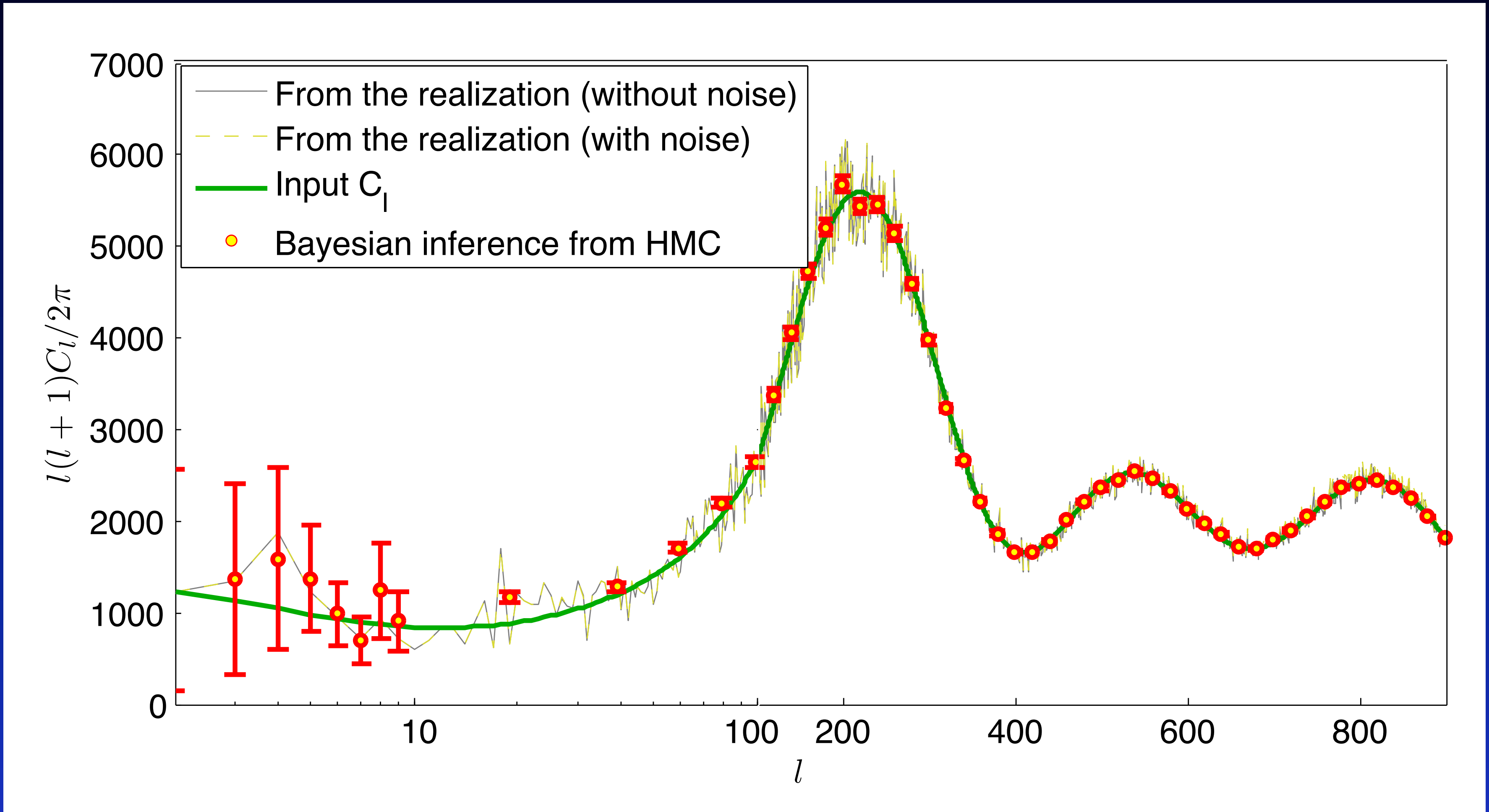

… so, the method does as well (or even better) than Gibbs Sampling

Tests on SI maps: BipoSH

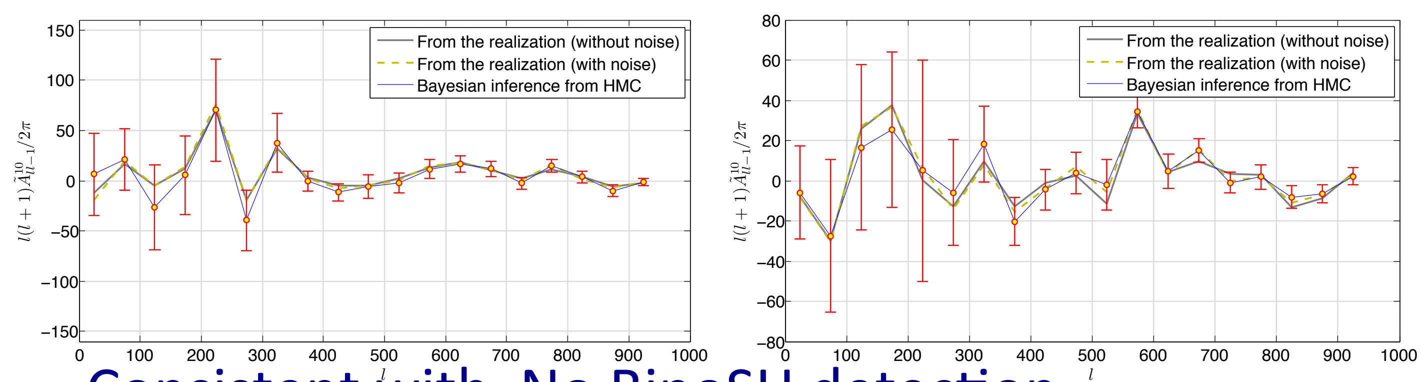

Consistent with No BipoSH detection

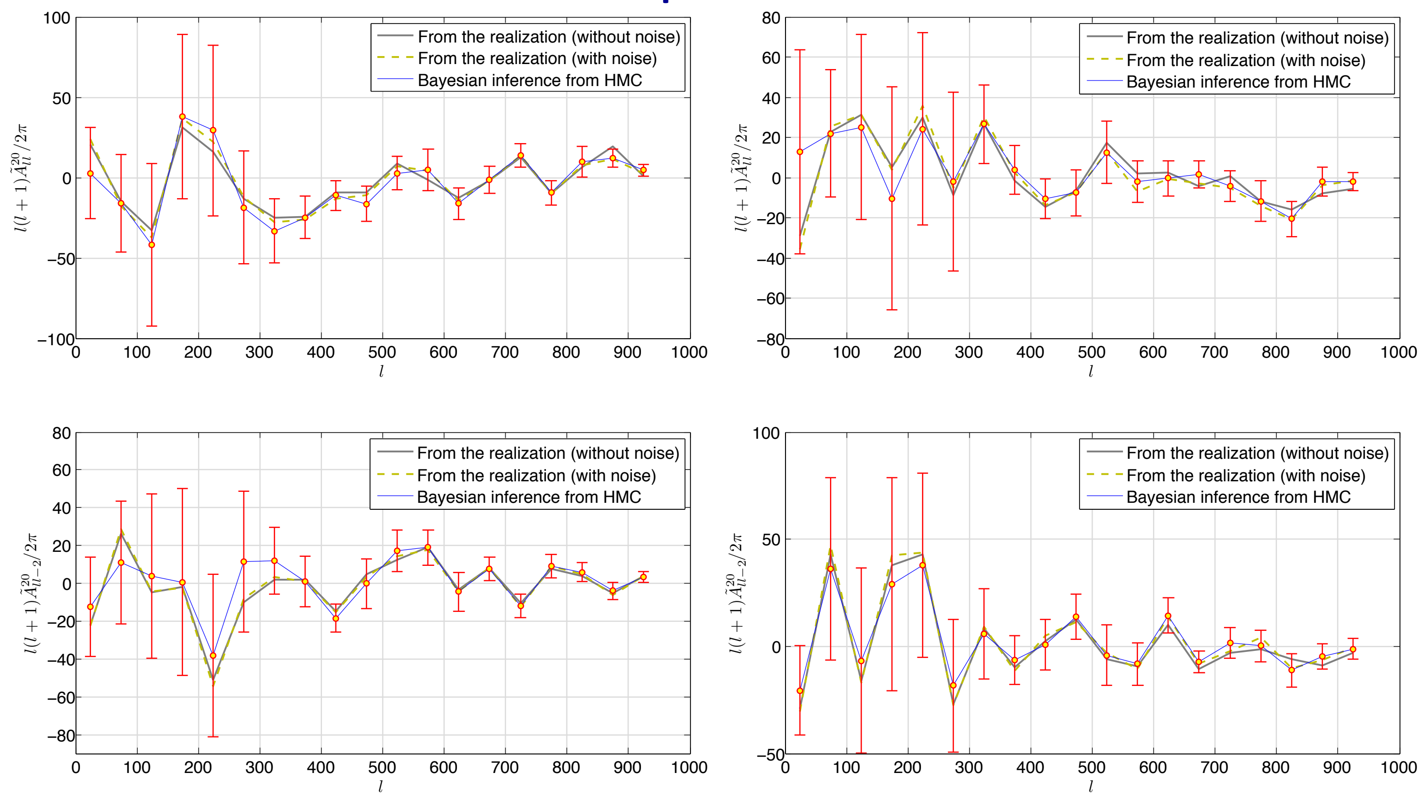

…. with complete posterior distributions

l = 7 | l = 70 | l = 700

C_l

BipoSH L = 1

BipoSH L= 2

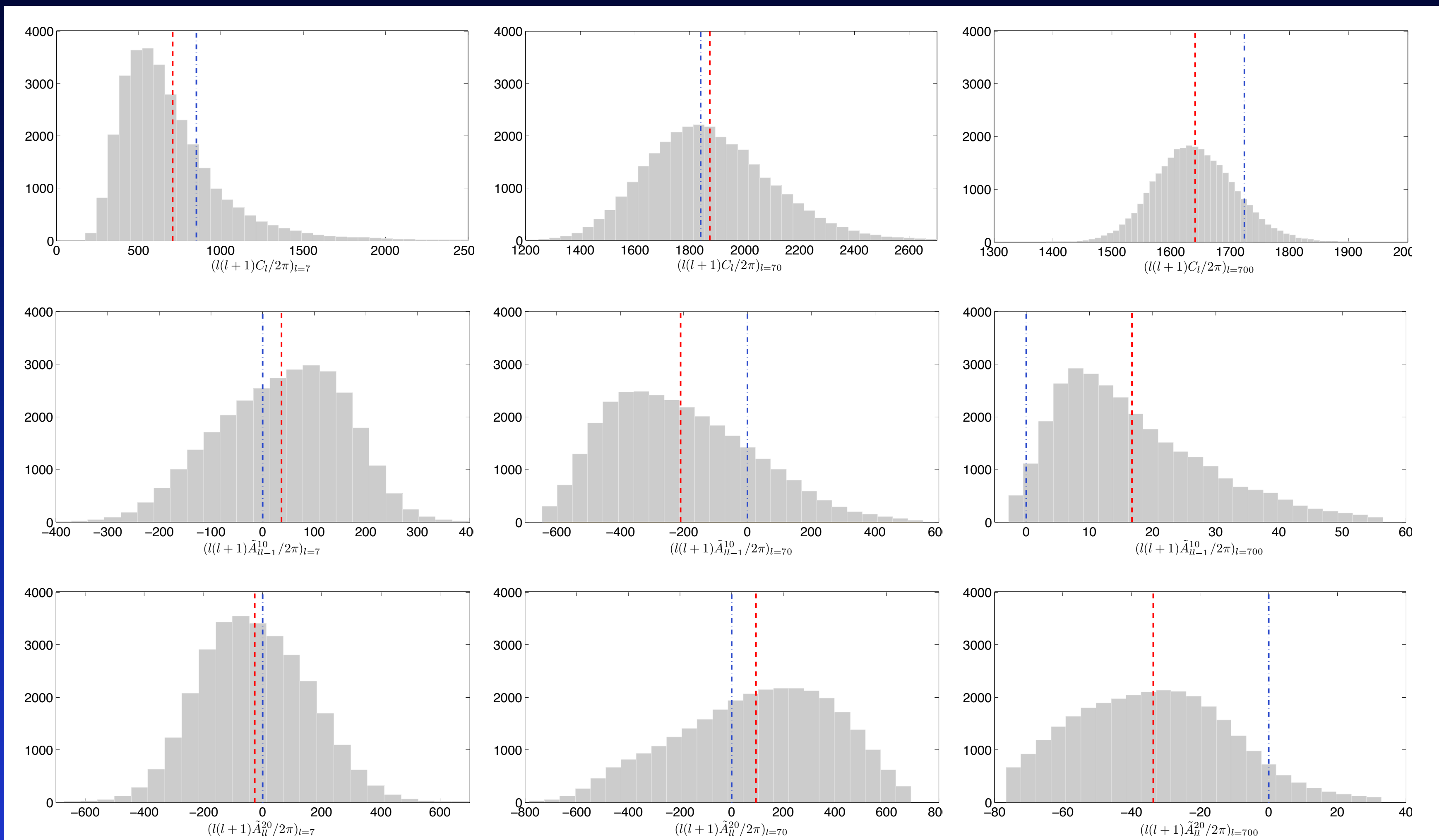

Bayesian HMC : Doppler boost

BipoSH Spectra
L=1

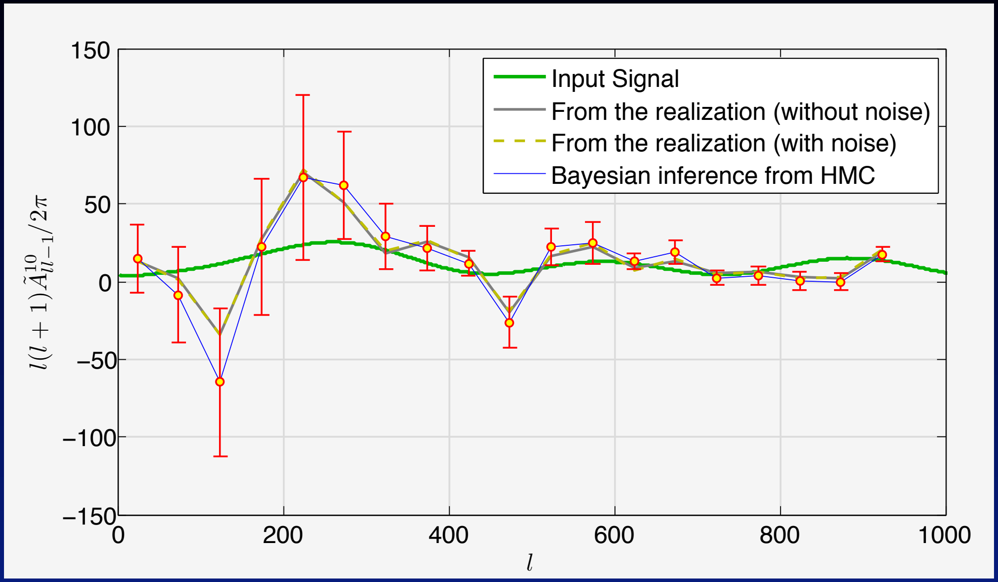

Used simulated
Doppler boosted
CMB maps using
CoNIGS
(Suvodip Mukherjee)

Posterior distribution of Boost parameter

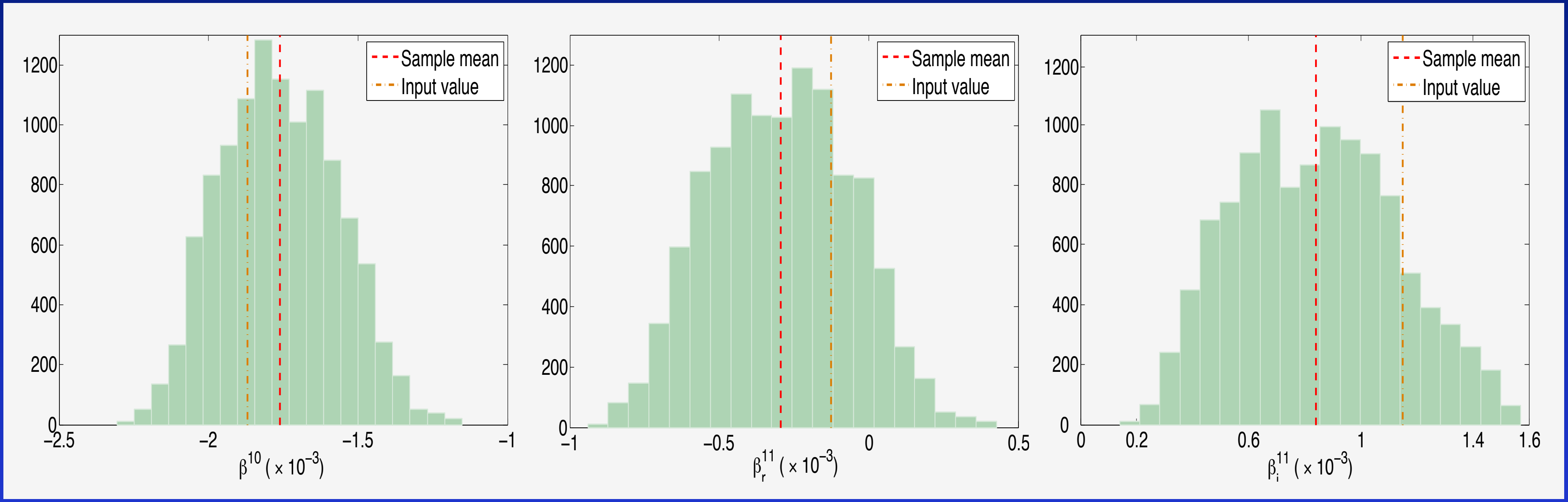

Bayesian HMC : CHA

$$\Delta T(\hat{n}) = [1 + A\ (\hat{p}.\hat{n})]\ \Delta T^{\mathrm{SI}}(\hat{n})$$

$$A = 1.5\sqrt{\frac{m_1}{\pi}}$$

$$m_1 = \frac{|m_{10}|^2 + |m_{11}|^2 + |m_{1-1}|^2}{3}$$

BipoSH Spectra
L=1

Used simulated Doppler boosted CMB maps using CoNIGS (Suvodip Mukherjee)

Posterior distribution of m_{10}, m_{11}, m_{1-1} parameters

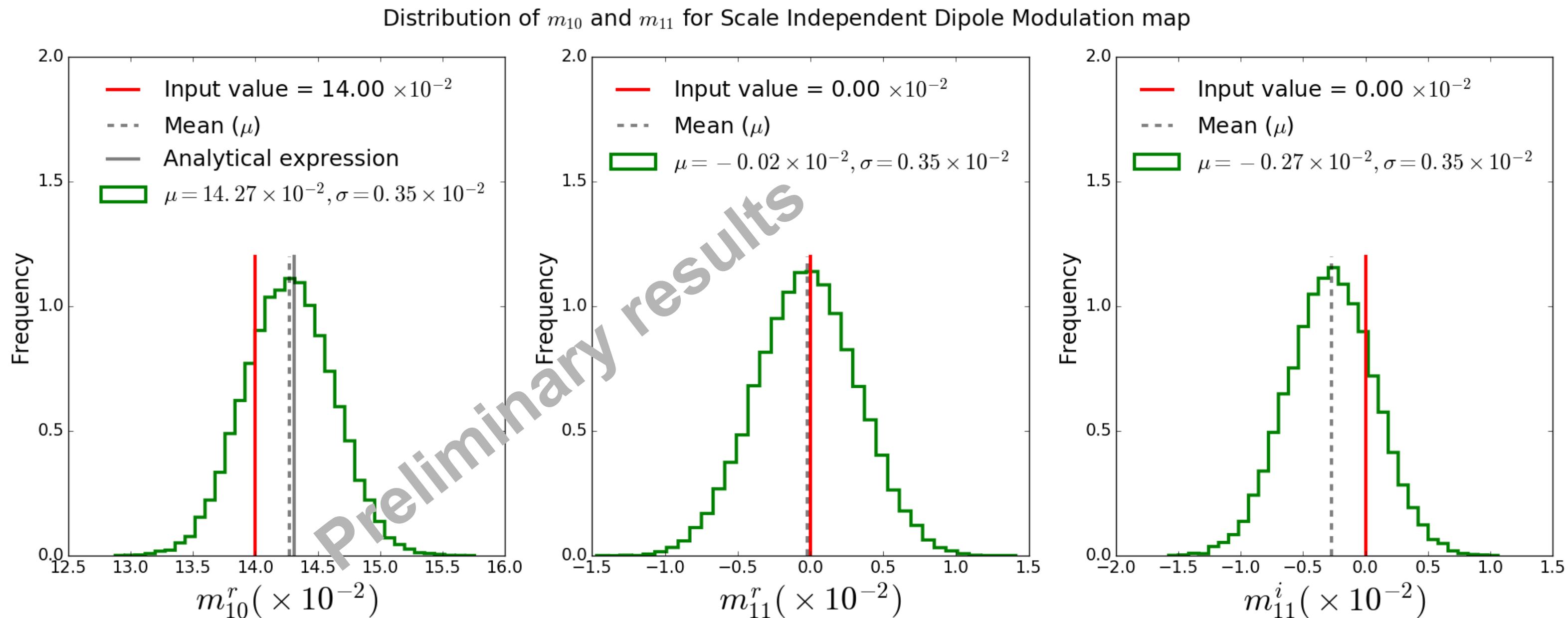

Cosmic Hemispherical asymmetry

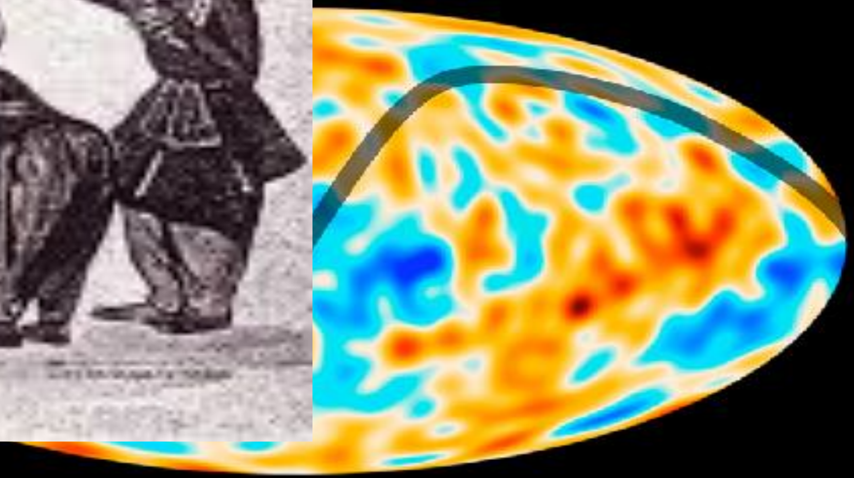

CHA: An enigma

Many Theoretical ideas

- Inflationary paradigm

  Erickcek, Kamionkowski & Carroll, (2008); Erickcek, Carroll & Kamionkowski, (2008); Donoghue, Dutta & Ross (2009); Erickcek, Hirata & Kamionkowski, (2009); Mazumdar, Wang, (2013); McDonald, (2014); Abolhasani et al., (2014); Liu, Guo & Piao (2014); Jazayeri,(2014); Liu et al. (2014).; Lyth, (2015); **Mukherjee & Souradeep (2015),** Kothari, Rath & Jain, (2015); Kothari et al., (2015); Wang et al. (2015)

- Dark Energy

  Perivolaropoulos (2014);
  Dai et al. (2013)

- Cosmic String

  Ringeval et al. (2016)

Observational Claims

- WMAP

F. K. Hansen et al. (2004).
H. K. Eriksen et al., (2004).
Godan (2007)
Hoftuft et al (2009)

- Planck

F. Paci et al. (2013)
Flender et al. (2013)
Planck-13 (2014)
Y. Akrami et al., (2014)
Quartin et al. (2015)
S. Aiola et al. (2015)
Planck-15, (2016)

Fast roll inflation with initial inhomogeneities

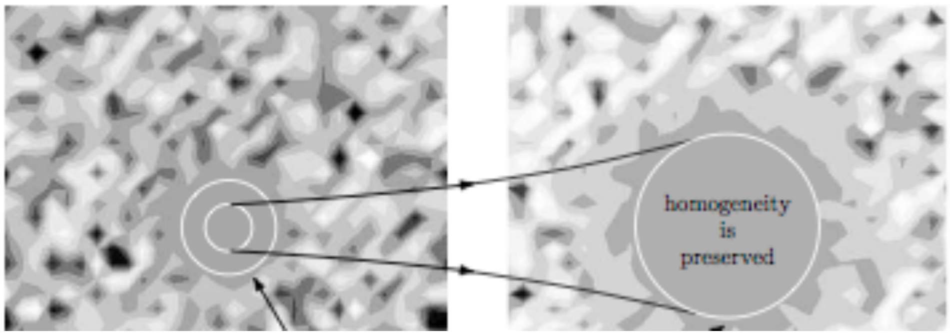

$$H(\hat{n},\tilde{\Phi}) = H_b(\Phi)[1+\chi(\tilde{\Phi})\,\hat{p}.\hat{n}],$$
$$H'(\hat{n},\tilde{\Phi}) = H_b'(\Phi)[1+\xi(\tilde{\Phi})\,\hat{p}.\hat{n}].$$
$$\chi = 2\sqrt{\pi\epsilon_H}\,\frac{\delta\Phi}{m_{pl}},$$
$$\xi = 2\sqrt{\pi}\,\frac{\eta_H}{\sqrt{\epsilon_H}}\,\frac{\delta\Phi}{m_{pl}}.$$

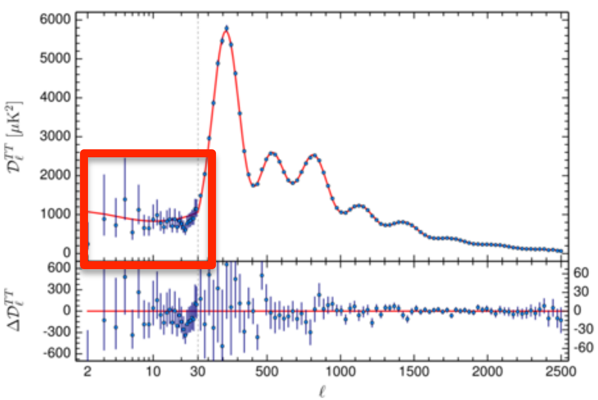

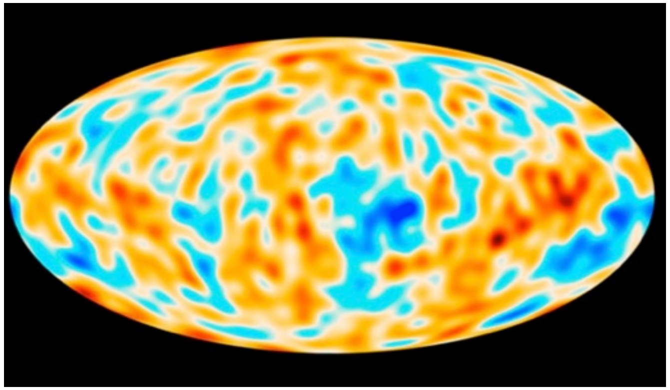

$$\tilde{P}_{s,t}(k,\hat{n}) = P_{s,t}(k)\left[1 + D^{s,t}\hat{p}.\hat{n} + Q^{s,t}(\hat{p}.\hat{n})^2\right],$$

In Single field inflation model, effect in tensor anisotropies is <0.05%

$$D^s(\tau) = 4\chi - 2\xi,\ Q^s(\tau) = 6\chi^2 - 8\chi\xi + 3\xi^2,\ D^t(\tau) = 2\chi \text{ and } Q^t(\tau) = \chi^2.$$

CHA in B modes from scalar perturbations : An inevitable window

Mukherjee and Souradeep
Phys. Rev. Lett. 116, 221301 (2016)

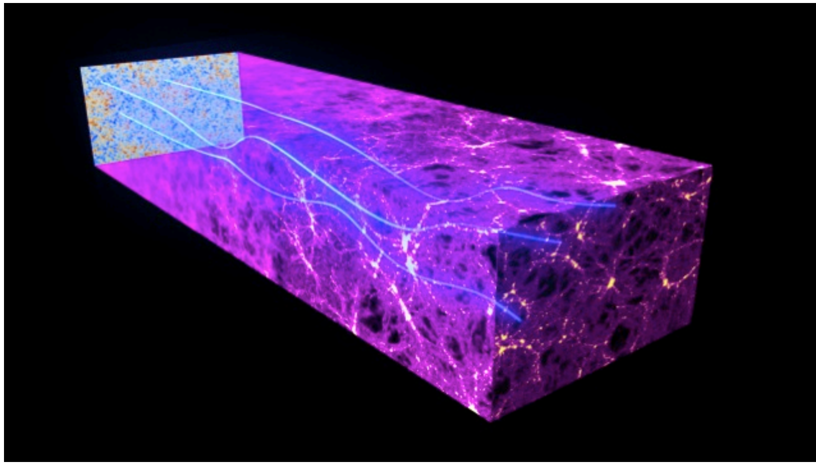

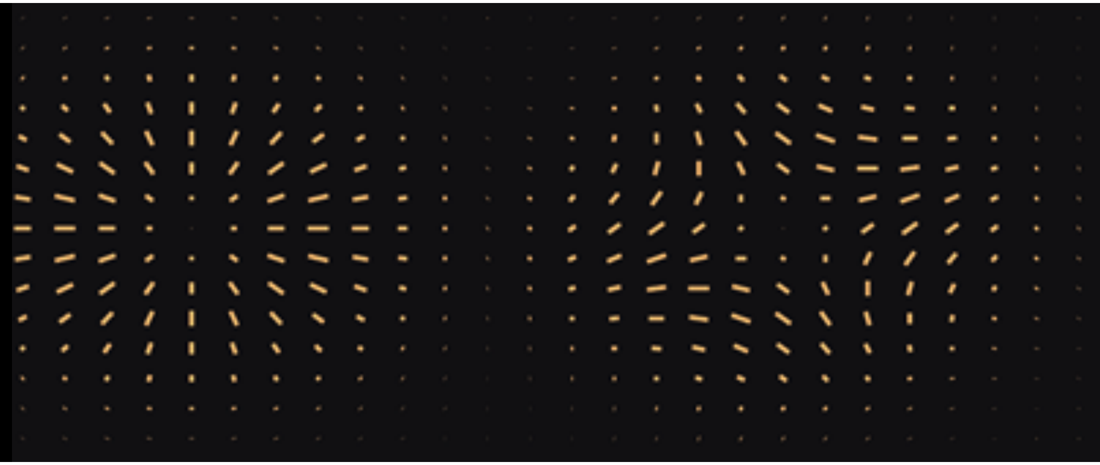

$$_{\pm s}\tilde{X}(\hat{n}) = {}_{\pm s}X(\hat{n} + \vec{\bigtriangledown}\Psi)$$

$$_{\pm 2}\tilde{X}(\hat{n}) = (1 + \alpha_{s,t}\,\hat{p}.\hat{n})_{\pm 2}X(\hat{n}) + \bigtriangledown_i((1 + \alpha_{s,t}\,\hat{p}.\hat{n})\Psi(\hat{n}))\bigtriangledown^i((1 + \alpha_{s,t}\,\hat{p}.\hat{n})_{\pm 2}X(\hat{n})) + \frac{1}{2}\Big[\bigtriangledown_i((1 + \alpha_{s,t}\,\hat{p}.\hat{n})\Psi(\hat{n}))\bigtriangledown_j((1 + \alpha_{s,t}\,\hat{p}.\hat{n})\Psi(\hat{n}))\Big]\Big[\bigtriangledown^i\bigtriangledown^j((1 + \alpha_{s,t}\,\hat{p}.\hat{n})_{\pm 2}X(\hat{n}))\Big]$$

CHA in B modes from scalar perturbations

Mukherjee and Souradeep
Phys. Rev. Lett. 116, 221301 (2016)

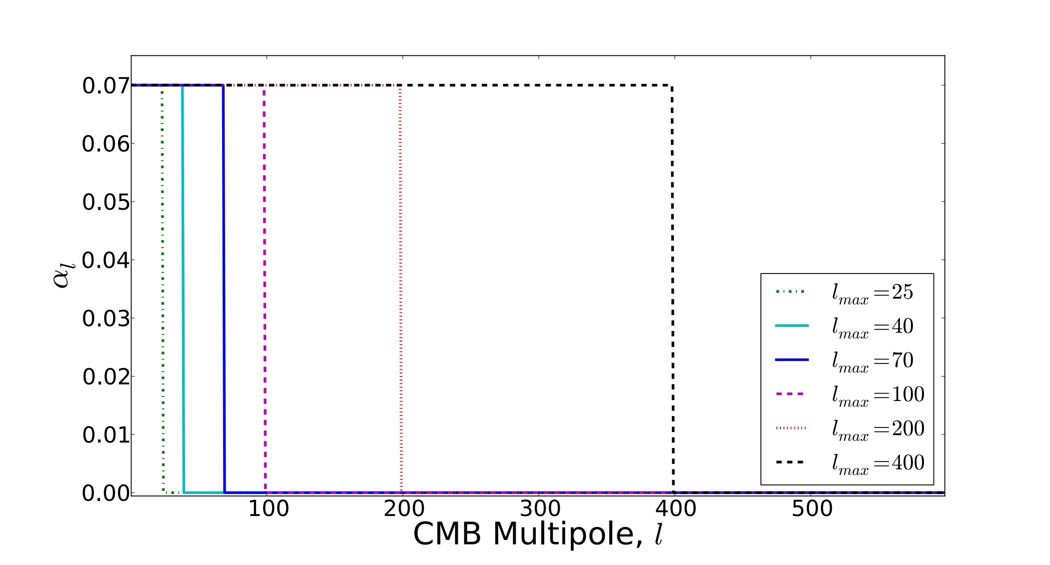

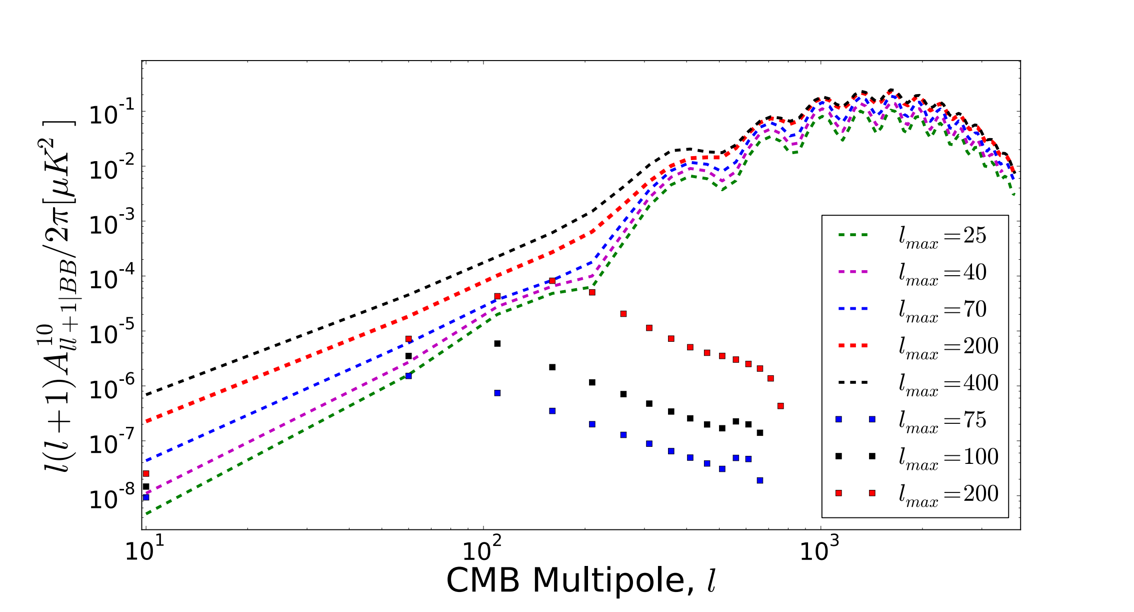

Mukherjee and Souradeep
Phys. Rev. Lett. 116, 221301 (2016)

$$\left\langle {}_{\pm2}\tilde{X}_{lm}\,{}_{\pm2}\tilde{X}^{*}_{l'm'}\right\rangle = \sum_{K}\left[\alpha^{1K} C^{EE}_{l'}\,{}_{\pm2}G^{mm'K}_{ll'1} + \alpha^{*1K} C^{EE}_{l}\,{}_{\pm2}G^{*m'mK}_{l'l1}\right]$$

$$+ \sum_{\substack{Jl_1l_2\\KNm_1m_2}} C^{\Psi\Psi}_{l_1} C^{EE}_{l_2}\left[\alpha^{1K}\,{}_{\pm2}H^{*m'm_1m_2}_{l'l_1l_2}\left({}_{\pm2}H^{mNm_2}_{lJl_2}\,{}_{0}R^{NKm_1}_{J1l_1} + {}_{\pm2}H^{mm_1N}_{ll_1J}\,{}_{\pm2}R^{NKm_2}_{J1l_2}\right)\right.$$

$$\left. + \alpha^{*1K}\,{}_{\pm2}H^{mm_1m_2}_{ll_1l_2}\left({}_{\pm2}H^{*m'Nm_2}_{l'Jl_2}\,{}_{0}R^{*NKm_1}_{J1l_1} + {}_{\pm2}H^{*m'm_1N}_{l'l_1J}\,{}_{\pm2}R^{*NKm_2}_{J1l_2}\right)\right]$$

$$+ \sum_{\substack{Jl_1\\KNm_1}} C^{\Psi\Psi}_{l_1}\left[\alpha^{1K} C^{EE}_{l'}\left({}_{\pm2}I^{mNm_1m'}_{lJl_1l'}\,{}_{0}R^{NKm_1}_{J1l_1} + {}_{\pm2}I^{mm_1Nm'}_{ll_1Jl'}\,{}_{0}R^{NKm_1}_{J1l_1} + {}_{\pm2}I^{mm_1m_1N}_{ll_1l_1J}\,{}_{\pm2}R^{NKm'}_{J1l'}\right)\right.$$

$$\left. + \alpha^{*1K} C^{EE}_{l}\left({}_{\pm2}I^{*m'Nm_1m}_{l'Jl_1l}\,{}_{0}R^{*NKm_1}_{J1l_1} + {}_{\pm2}I^{*m'm_1Nm}_{l'l_1Jl}\,{}_{0}R^{*NKm_1}_{J1l_1} + {}_{\pm2}I^{*m'm_1m_1N}_{l'l_1l_1J}\,{}_{\pm2}R^{*NKm}_{J1l}\right)\right]$$

$$+ \sum_{\substack{Jl_1l_2\\KNm_1m_2}} C^{\Psi\Psi}_{l_1} C^{EE}_{l_2}\left[\alpha^{1K}\left({}_{\pm2}I^{m'm_1m_1m_2}_{l'l_1l_1l_2}\,{}_{\pm2}G^{mm_2K}_{ll_21}\right) + \alpha^{*1K}\left({}_{\pm2}I^{mm_1m_1m_2}_{ll_1l_1l_2}\,{}_{\pm2}G^{m'm_2K}_{l'l_21}\right)\right]$$

$${}_{\pm2}G^{mm_1m_2}_{ll_1l_2} = \int d^2\hat{n}\left({}_{\pm2}Y_{l_1m_1}(\hat{n})Y_{l_1m_1}(\hat{n})\,{}_{\pm2}Y^{*}_{lm}(\hat{n})\right);$$

$${}_{\pm2}H^{mm_1m_2}_{ll_1l_2} = \int d^2\hat{n}\left(\nabla_i\, Y_{l_1m_1}(\hat{n})\,\nabla^i\,{}_{\pm2}Y_{l_2m_2}(\hat{n})\,{}_{\pm2}Y^{*}_{lm}(\hat{n})\right),$$

$${}_{\pm2}I^{mm_1m_2m_3}_{ll_1l_2l_3} = \frac{1}{2}\int d^2\hat{n}\left(\nabla^i\, Y_{l_1m_1}(\hat{n})\,\nabla^i\, Y_{l_2m_2}(\hat{n})\,\nabla_i\,\nabla_j\,{}_{\pm2}Y_{l_2m_2}(\hat{n})\,{}_{\pm2}Y^{*}_{lm}(\hat{n})\right);$$

$${}_{\pm s}R^{mm_1m_2}_{ll_1l_2} = \frac{\Pi_{l_1l_2}}{\sqrt{4\pi}\Pi_l} C^{l\,\pm s}_{l_1\,0\,l_2\,\pm s}\, C^{lm}_{l_1\,m_1\,l_2\,m_2}$$

Mukherjee and Souradeep
Phys. Rev. Lett. 116, 221301 (2016)

$$
\begin{aligned}
A^{10}_{ll+1|BB} = & \\
& \sum_{Jl_1l_2}^{(l_1)_{max}} \frac{\alpha^{10}_{l_1}}{2\sqrt{4\pi}} \Bigg[C^{\Psi\Psi}_{l_1}[C^{EE}_{l_2} - (-1)^{l+1+l_1+l_2} C^{EE}_{l_2}] \\
& \Bigg[M_{Jl_2l} M_{l_1l_2l+1} C^{J0}_{10l_10} C^{l\,2}_{J0l_2\,2} C^{l+1\,2}_{l_10l_2\,2} \Pi_{l_1Jl_2l_2} \mathcal{W}_{l_1l_2l+1J1l} \Bigg] + \\
& C^{\Psi\Psi}_{l_1}[C^{EE}_{l_2} - (-1)^{l+1+J+l_2} C^{EE}_{l_2}] \\
& \Bigg[M_{l_1l_2l} M_{Jl_2l+1} C^{J0}_{10l_10} C^{l\,2}_{l_10l_2\,2} C^{l+1\,2}_{J0l_2\,2} \Pi_{l_1Jl_2l_2} \mathcal{W}_{l_1l_2lJ1l+1} \Bigg] \Bigg] + \\
& \sum_{Jl_1l_2}^{(l_2)_{max}} \frac{\alpha^{10}_{l_2}}{2\sqrt{4\pi}} \Bigg[C^{\Psi\Psi}_{l_1}[C^{EE}_{l_2} - (-1)^{l+1+l_1+l_2} C^{EE}_{l_2}] \\
& \Bigg[M_{l_1Jl} M_{l_1l_2l+1} C^{J2}_{10l_22} C^{l\,2}_{l_10J\,2} C^{l+1\,2}_{l_10l_2\,2} \Pi_{l_1l_1Jl_2} \mathcal{W}_{l_2l_1l+1J1l} \Bigg] + \\
& C^{\Psi\Psi}_{l_1}[C^{EE}_{l_2} - (-1)^{l+1+l_1+J} C^{EE}_{l_2}] \\
& \Bigg[M_{l_1l_2l} M_{l_1Jl+1} C^{J2}_{10l_22} C^{l\,2}_{l_10l_2\,2} C^{l+1\,2}_{l_10J\,2} \Pi_{l_1l_1Jl_2} \mathcal{W}_{l_2l_1lJ1l+1} \Bigg] \Bigg],
\end{aligned}
$$

$$
A^{10}_{ll+1|BB} = \sum_{l_1}^{(l_1)_{max}} \alpha^{10}_{l_1} S^{10}_{ll+1l_1},
$$

$$
\text{where, } \mathcal{W}_{l_2l_1lJ1l'} = \begin{pmatrix} l_2 & l_1 & l' \\ l & 1 & J \end{pmatrix}; \; M_{l_1l_2l} = \frac{1}{2\sqrt{4\pi}}[l_1(l_1+1) + l_2(l_2+1) - l(l+1)];
$$

$$
\Pi_{l_1l_2\ldots l_n} = \sqrt{(2l_1+1)(2l_2+1)\ldots(2l_n+1)}
$$

CHA in B modes from scalar perturbations

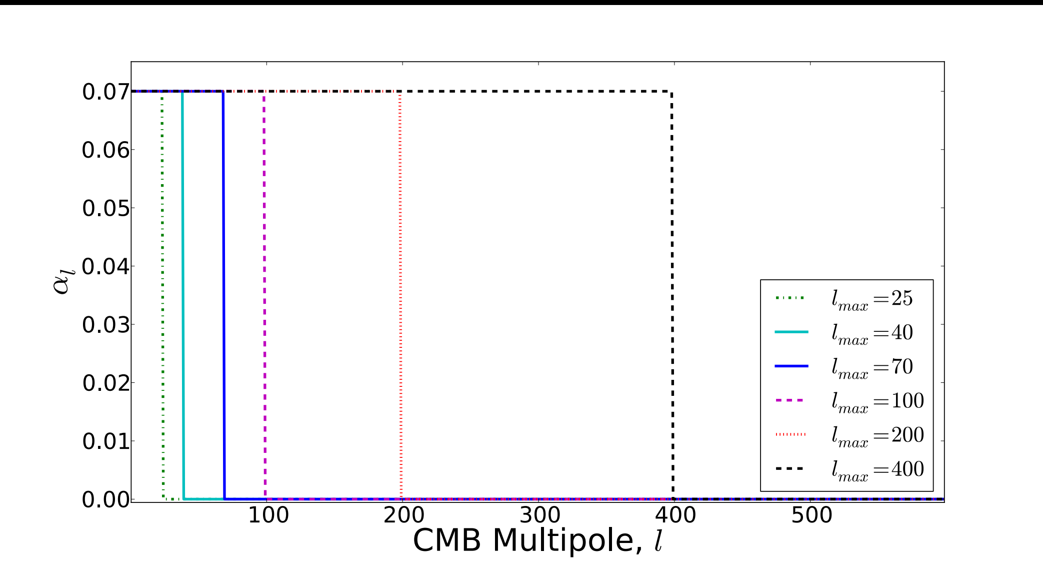

Mukherjee and Souradeep
Phys. Rev. Lett. 116, 221301 (2016)

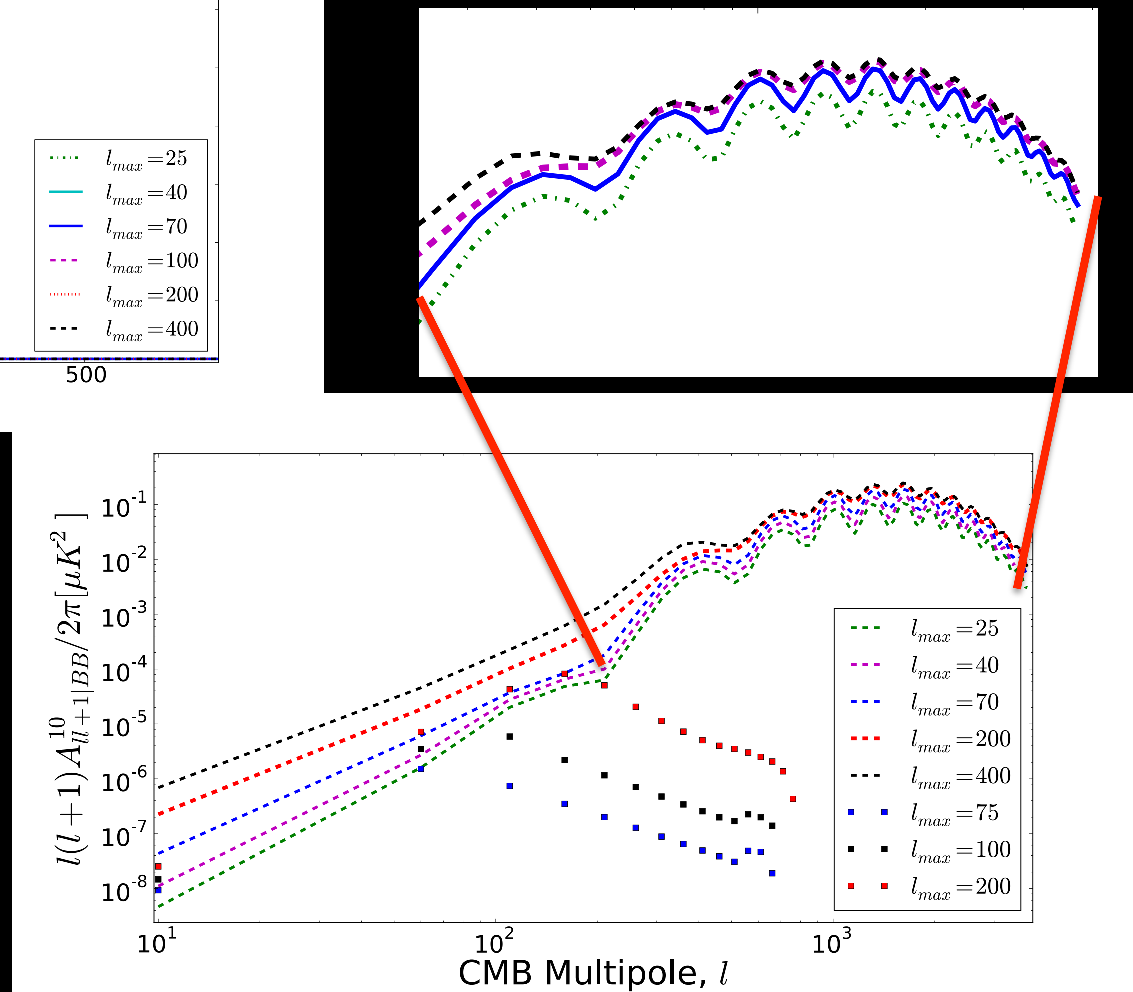

CHA in B modes at small angular scales

A new window to put bounds on CHA of primordial origin

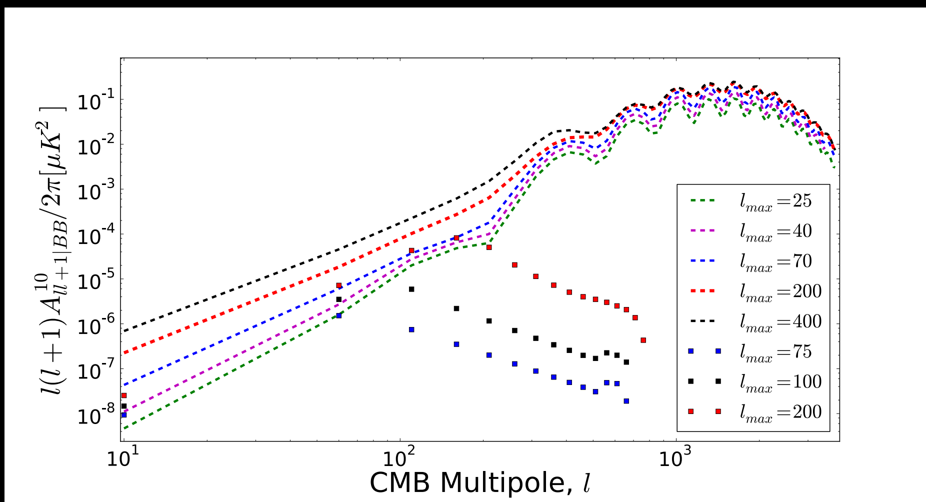

Mukherjee and Souradeep
Phys. Rev. Lett. 116, 221301 (2016)

Extent of CHA in lensing (l_{max})	Cumulative noise	Signal to Noise Ratio (SNR)
25	0.054	1.28
30	0.0456	1.53
40	0.034	2.04
70	0.02	3.46

Universe, yours to explore !

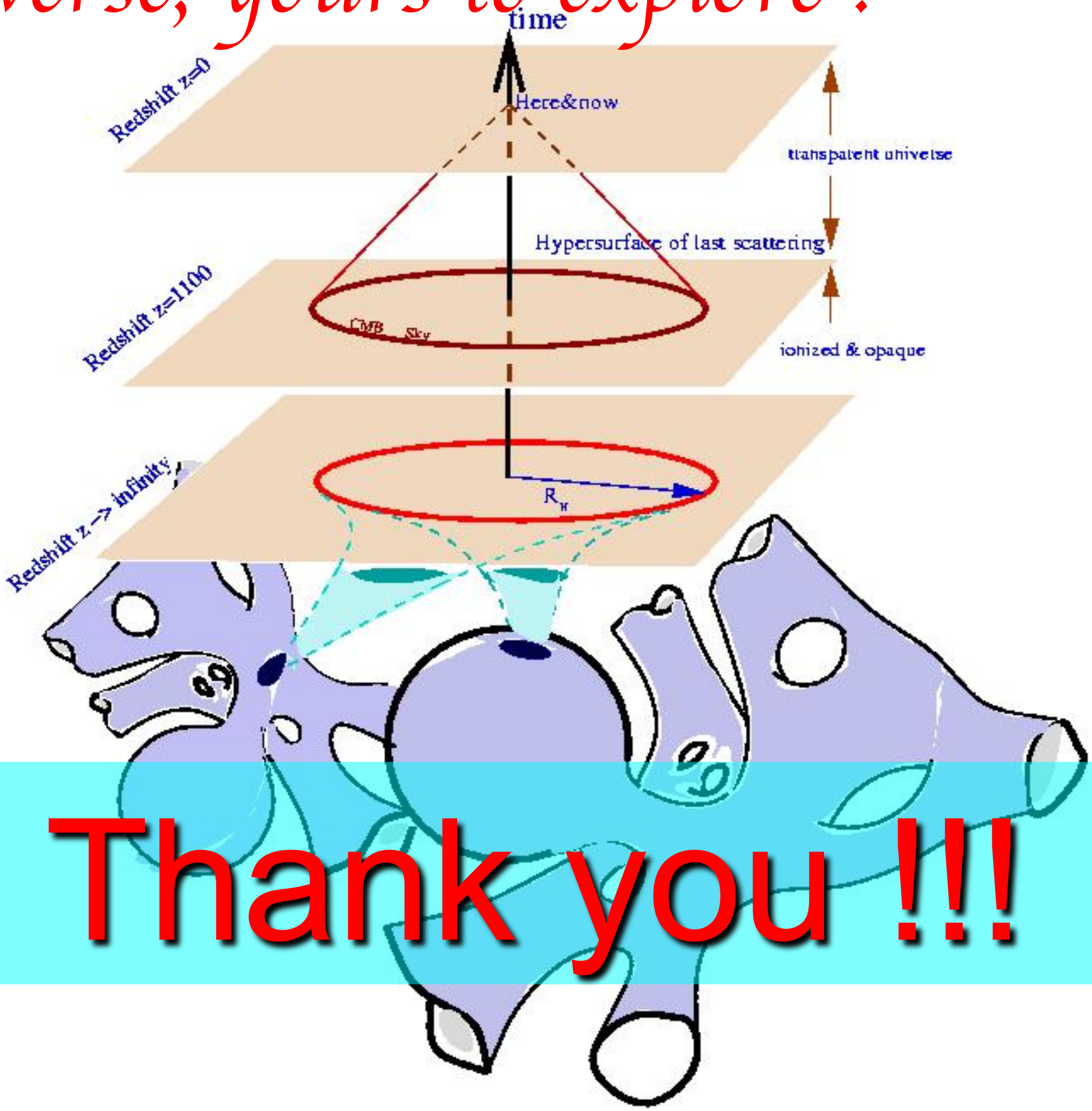

Thank you !!!